약학박사 학위논문

Regulation of epithelial-mesenchymal transition in tamoxifen-resistant human breast cancer by ERα66/ERα36 and Notch4/STAT3 pathways

타목시펜 저항성 인간 유방암세포에서 ERα66/ERα36 및 Notch4/STAT3 경로를 통한 상피간엽이행 조절

2017년 2월

서울대학교 대학원

약학과 약물학 전공

BUI THU QUYEN

Regulation of epithelial-mesenchymal transition in tamoxifen-resistant human breast cancer by ERα66/ERα36 and Notch4/STAT3 pathways

타목시펜 저항성 인간 유방암세포에서 ERα66/ERα36 및 Notch4/STAT3 경로를 통한 상피간엽이행 조절

지도교수 강 건 욱

이 논문을 약학박사 학위논문으로 제출함

2017 년 02 월

서울대학교 대학원

약학과 약물학 전공

BUI THU QUYEN

부이뚜귀엔의 약학 박사 학위 논문을 인준함

2017 년 02 월

위 원 장 김 상 건 (인)

부위원장 정 연 석 (인)

위 원 김 상 겸 (인)

위 원 김 형 식 (인)

위 원 강 건 욱 (인)

Abstract

Regulation of epithelial-mesenchymal transition in tamoxifen-resistant human breast cancer by ERα66/ERα36 and Notch4/STAT3 pathways

BUI THU QUYEN

College of Pharmacy

The Graduate School

Seoul National University

Breast cancer is one of the most common malignant tumors and leading causes of cancer-related death in women. Among all types of breast cancer, 70% are estrogen receptor alpha-positive (ERα (+)) breast cancer. Hormonal therapy to block the ERα pathway is high effective to ERα (+) breast cancer and tamoxifen (TAM) has emerged as the most effective drug. However, breast cancer cells continuous exposure to TAM recur acquired tamoxifen-resistant despite the initial responsive, subsequently stimulate cell proliferation, migration, invasion and metastasis. We previously demonstrated that tamoxifen (TAM)-resistant human breast cancer (TAMR-MCF-7) cells showed increased expression of mesenchymal marker proteins compared to the

parent MCF-7 cells.

ERα is a 66kDa, ligand-induced nuclear receptor transcription factor and it functionally plays important role in mediating many processes in human breast cancer. Several studies have reported the downregulation of ERα66 during the development of acquired TAM resistant breast cancer. It has been recently identified and cloned a 36kDa novel variant of ERα66, ERα36, which lacks both transcriptional activation domains (AF-1 and AF-2), but retains a truncated ligand-binding domain and an intact DNA-binding domain of the full-length ERα66. While ERα66 is mainly distributed in the nucleus, ERα36 predominantly localizes in the cytoplasm and plasma membrane. We observed the expression loss of ERα66 and elevation of ERα36 in TAM-resistant breast cancer (TAMR-MCF-7) compared to parental MCF-7 cells. In this study, we evaluated the role of ERα 66 and ERα36 in the progression of acquired TAM resistance and EMT process in breast cancer. Our study revealed that ERα36 is a key signaling factor for estrogen-independent cell proliferation and tumorigenesis of tamoxifen-resistant breast cancer. Overexpression of ERα36 resulted in loss of ERα66, subsequently participating in acquisition of EMT. ERα36 seems to be involved in EMT process of TAMR-MCF7 cells by inhibiting ERα66 expression. However, the murine model of hepatic metastases performed via a hemispleen injection demonstrated that ERα36-overexpressing MCF-7 cells failed to cause metastatic tumor burden in liver though this cell type also displayed features of EMT-like phenotype similar to TAMR-MCF-7 cells. Moreover, overexpression of ERα66 in TAMR-MCF-7 cells could reverse the EMT to MET characterized by restoring the epithelial marker expression, E-cadherin. Likewise, overexpression of

ERα66 in other ERα66-negative breast cancer cells such as MDA-MB-231, SKBR3 resulted in suppression of EMT and cell migration. However, spleen injection for liver metastases experiments revealed the same micrometastatic hepatic tumor burden between control TAMR-MCF-7 cells (TAMR-GFP) and ERα66-overexpressing TAMR-MCF-7 cells (TAMR-ER66). Thus, ERα66 function plays as a crucial factor in differentiation and maintenance of normal epithelial architecture.

Notch is functionally important in the promotion of EMT during both development and progression of tumor. Notch1 and Notch4 have been reported as prognostic markers in human breast cancer. Here, we indicated that Notch4, but not Notch1, plays a critical role in the regulation of EMT signaling in TAMR-MCF-7 cells. Notch4 suppression by either Notch inhibitors or Notch4 siRNA attenuated EMT signaling. Tyrosine-phosphorylated STAT3 protein is known as a crucial signaling molecule in the regulation of tumorigenesis and metastasis. We found that TAMR-MCF-7 cells exhibited constitutive STAT3 phosphorylation, and Notch inhibition reduced the level of activated STAT3 in TAMR-MCF-7 cells. Our study also revealed that STAT3 bound physically with Notch4-intracellular domain (Notch4-ICD) but not the full-length of Notch4. Intrasplenic injection model of liver metastases was performed using TAMR-MCF-7 cells. Mice injected with N-[N-(3,5-Difluorophenacetyl)-L-alanyl]-S-phenyl glycine t-butyl ester (DAPT; 10 mg/kg; an inhibitor of γ-secretase) formed smaller splenic tumors and showed a reduced micrometastatic tumor burden in their livers compared with the control group treated with vehicle. This study reported for the first time the physical binding between STAT3 and Notch4-ICD and this interaction may

play an important role in EMT progression during acquired tamoxifen-resistant breast cancer.

Collectively, this study proposes two signaling pathways which are responsible for epithelial mesenchymal transition (EMT) phenotype during acquired tamoxifen-resistant human breast cancer.

keywords : EMT, Notch4, ERα66, ERα36, tamoxifen-resistant breast cancer

Student Number **: 2012-30773**

Contents

List of tables

List of figures

List of abbreviations

3D: Three-dimensional
Akt: Protein kinase B
AP-1: Activator protein-1
CSCs: Cancer stem cells
C/D FBS: charcoal-stripped, steroid-depleted FBS
DAPI: 4 ,6-Diamidino-2-Phenylindole
DAPT: N-[N-(3,5-Difluorophenacetyl)-L-alanyl]-S-phenylglycine t-butyl ester
DMEM: Dulbecco's modified Eagle's medium
DMFS: Distance metastasis-free survival
EMT: Epithelial-mesenchymal transition
ER: Estrogen receptor
ERα: Estrogen receptor alpha
ERα36, estrogen receptor alpha 36
ERα66, estrogen receptor alpha 66
ERE: Estrogen response element
ERK: extracellular signal-regulated kinase
FBS: Fetal bovine serum
GEO: Gene Expression Omnibus
GSK3 β: Glycogen synthase kinase 3 beta
H&E: hematoxylin and eosin
ICC: Immunocytochemistry
ICD: Intracellular domain
IHC: Immunohistochemistry
MET: Mesenchymal-epithelial transition
MMP2: Matrix metalloproteinase 2
NF-κB: Nuclear factor-kappa B
PBS: Phosphate buffered saline
PEG 400: Polyethylene glycol 400

PI3K: Phosphatidylinositide 3-kinase
PRF: Phenol red-free
SERMs: Selective estrogen receptor modulators
STAT3: Signal transducer and activator of transcription 3
RFS: Relapse-free survival
RT-PCR: Reverse transcription-polymerase chain reaction
TAM: Tamoxifen
TAMR: Tamoxifen resistant

I. INTRODUCTION

Breast cancer is the most common cancer in women worldwide which is multifaceted disease comprised of distinct biological subtypes with different prognostic and therapeutic implications [1,2]. Because of diversity of cause and clinical features, determining classification of breast cancer subtypes is important for treatment strategies. Breast cancer subtypes can be differentiated based on the expression on tumor cells of estrogen receptors (ER). About 70% of all breast cancers are estrogen receptor α (ERα)-positive (ERα(+)) which are likely to respond to endocrine therapies [2].

Targeting estrogen receptors has become the most effective approach for ERα(+) breast cancer therapy since endogenous estrogens are thought to play a vital role in breast cancer development. Selective estrogen receptor modulators (SERMs) such as tamoxifen and raloxifene are competitive inhibitors of estradiol at the estrogen receptor. These inhibitors act agonist or antagonist behavior depending on the tissue [3]. Additionally, estrogen production can be extremely blocked by inhibiting the conversion of steroidal precursors to estrogen using aromatase inhibitors such as anastrozole and letrozole [4].

Despite tamoxifen (TAM) showing clear benefits for the prevention and treatment of ERα66(+) breast cancer, continuous exposure to TAM confers drug resistance [5]. As a consequence, TAM resistance is a considerable limiting factor in the management of advanced breast cancer. Previous studies demonstrated increased cell motility *in vitro* and morphological distinctions between

TAM-resistant human breast cancer (TAMR-MCF-7) cells and their parent MCF-7 cells [5,6].

Epithelial mesenchymal transition (EMT) is a process by which epithelial cells lose their cell polarity and gain migratory and invasive properties to become mesenchymal stem cells [7]. As cells undergo EMT, they lose epithelial cell-cell coherence, reorganize their actin cytoskeleton, downregulate the expression of cell adhesion molecules such as E-cadherin and upregulate the expression of mesenchymal markers such as N-cadherin and vimentin [7]. In addition, the activities of matrix metalloproteinases (MMPs) such as MMP2 and MMP9 are elevated during EMT progression [8].

E-cadherin is a calcium-regulated homophilic cell-cell adhesion molecule and is expressed in surfaces of epithelial cells in regions of cell-cell contact known as adherens junctions [9]. The loss of E-cadherin causes the dedifferentiation and invasiveness of human cancers [10], indicating that E-cadherin is one of the hallmarks of invasive breast cancer phenotypes [11]. It has been reported that decreased levels of E-cadherin related to the distant metastasis and poor prognosis of breast cancer [12,13].

The status of ERα expression is a useful clinical biomarker for diagnosis and prognosis in breast cancer [2]. The typical ERα is a 66 kDa (here termed ERα66), ligand-induced transcription factor, characteristically detected in the cell nucleus by immunohistochemistry (IHC) in breast cancer specimens. Wang et al. has recently identified a 36 kDa novel isoform of ERα which have named as ERα36 [14]. ERα36 differs from full-length ERα66 since it lacks both of the two transcriptional activation domains (AF-1 and AF-2), but still retains the DNA-binding domain, and partial

dimerization and ligand-binding domains [14]. ERα36 possesses an extra, unique 27-amino-acid sequence which is replaced by the last 138 amino acids at C-terminus [15]. ERα36 fundamentally localizes in the plasma membrane and cytoplasm and responds to both estrogens and antiestrogens by inducing membrane-initiated signaling cascades, stimulating proliferation and possibly contributing to a more aggressive phenotype in breast carcinomas [15,16]. Summarizing from several reports, Table 1 demonstrated that ERα36 is highly expressed in ERα66-negative breast cancer cells (i.e., MDA-MB-231, MDA-MB-436 and SKBR3), and weaker detected in ERα66-positive breast cancer cells (i.e., MCF-7, H3396, and T47D) [16-19].

Table 1. Expression of ERα36 and ERα66 receptors in different breast cancer cell lines

ERα status	Cells	ERα36	ERα66
ERα positive	MCF-7 H3396 T47D	Low expression both in plasma membrane and cytoplasm	High expression both in nucleus and cytoplasm
ERα negative	MDA-MB-231 MDA-MB-436	High expression both in plasma membrane and cytoplasm	None
	SKBR-3		

IHC analyses of tumor specimens demonstrated that approximately 40% of ERα66-positive breast cancer patients also expressed ERα36 in their tumors, and this subset of patients was less likely to benefit from TAM treatment compared to those with

ERα66-positive/ERα36-negative tumors [20]. Furthermore, Li et al. reported that TAMR-MCF-7 cells possesses high levels of ERα36 and EGFR expression but nearly undetectable ERα66 expression [18]. It has also been revealed that ERα36 expression plays an important role in this growth status switch via overexpressing ERα36 expression in MCF-7 cells and knocking down ERα36 expression in TAMR-MCF-7 cells, which contributed to the generation of acquired TAM resistance [18].

One of the remaining questions is how hormonally responsive breast cancers progress to a more aggressive and hormonally independent phenotype. It is worth noticing that endocrine resistance is generally characterized by accelerated growth and initiated aggressive behavior, subsequently associated with changes of the morphological characteristics of cells undergoing EMT [5]. Our previous report also displayed that TAMR-MCF-7 cells are morphologically distinct and more invasive than their parental MCF-7 cells [6]. In this study, we try to answer the question “which forms of estrogen receptor alpha (ERα66 or ERα36) is/are important for EMT phenotype during acquired Tamoxifen-resistant human breast cancer cells?” Our study revealed that overexpression of ERα66 in TAMR-MCF-7 cells could reverse the EMT to MET characterized by rescue of E-cadherin expression. In addition, overexpression of ERα66 in other ERα66-negative breast cancer cells displayed significantly effect on suppression of EMT and cell migration. ERα36-overexpressing MCF-7 cells exhibited extreme reducion of ERα66 expression and showed the typical EMT phenotype, whereas ERα36-silencing TAMR-MCF7 cells did not cause significant difference in ERα66 level as well as migratory suppression compared

to control cells. Thus, ERα36 likely induced EMT progression of TAMR-MCF7 cells by inhibiting ERα66 expression. ERα66 plays a fundamental role in differentiation and maintenance of epithelial characteristics.

Upregulation of Notch receptors and their ligands has been reported in several types of cancer cells, including breast cancer [21]. The Notch family comprises four receptors, Notch1, 2, 3 and 4 [22]. Notch1 and Notch4 are required for cell proliferation and stimulate matrix invasion in both ERα-negative and -positive breast cancer cells [23]. Moreover, constitutively active forms of Notch1 and Notch4 stimulate the transformation of normal human mammary epithelial cells *in vitro* [24,25]. Consistent with this finding, activation of Notch1 [25] or Notch4 [24] can cause mammary carcinogenesis in mice.

A number of stimuli and transcription factors have emerged as potent EMT drivers during normal development and cancer. Several studies have indicated the Notch signaling pathway as a crucial regulator in the induction of EMT and metastasis [24,26]. Notch ligand binding to an adjacent Notch receptor activates Notch signaling and leads to the morphology and phenotype consistent with mesenchymal transformation [26]. Upon activation, the Notch receptor is cleaved and undergoes conformational changes in which the Notch intracellular domain (ICD) is released through a cascade of proteolytic cleavages by metalloproteases, tumor necrosis factor-α-converting enzyme and the γ-secretase complex [26,27]. Accordingly, γ-secretase inhibition may prevent Notch-induced EMT in cancer cells. Notch4 activation significantly increases the tumorigenic potential of mammary epithelial cells by changing their morphogenetic properties

[28]. Yun et al. revealed that PKCα-overexpressing T47D cells showing TAM-resistant phenotype expressed high levels of Notch4, but not of Notch1 [29]. Notch4 is up-regulated in TAM-resistant MCF-7 breast cancer cells which possessed more invasive and migratory phenotype compared to wild type MCF-7 cells [30].

Endogenous activity of the Notch signaling pathway is critical for activation of signal transducer and activator of transcription 3 (STAT3) in neuroepithelial cells [31]. STAT3 is frequently activated in many human cancer types, including breast cancer [32]. Tumorigenic STAT3 activation is often associated with increased malignant cancer behaviors, including uncontrolled growth, EMT, migration, invasion, metastasis and therapeutic resistance [33,34]. Here, we observed that basal expression and activity of Notch4 were amplified in TAMR-MCF-7 cells, and we investigated the role of Notch4/STAT3 signaling in EMT of TAM-resistant human breast cancer, and the potential of Notch inhibitors in the suppression of the metastatic tumor burden *in vivo*.

In this study, we introduce that ERα66 and Notch4/STAT3 signaling pathways are responsible for epithelial mesenchymal transition (EMT) phenotype during acquired tamoxifen-resistant human breast cancer.

II. MATERIALS AND METHODS

1. Antibodies and reagents

Anti-E-cadherin and anti-N-cadherin antibodies were purchased from BD Transduction (San Jose, CA). Anti-Snail antibody was supplied from Abcam (Cambridge Science Park, UK). Anti-Notch1, anti-Notch4 and phospho-STAT3, anti-c-Jun, anti-c-Fos, anti-JunB, anti-JunD antibodies were obtained from Cell Signaling Technology (Danvers, MA). Anti-P65, anti-Notch1 (for immunohistochemistry), anti-Notch4 (for immunohistochemistry), anti-MMP2 and anti-ERα66 antibodies were obtained from Santa Cruz Biotechnology (Santa Cruz, CA). Anti-ERα36 antibody (CY1109) was supplied from Cell Applications (San Diego). Horseradish peroxidase-conjugated, donkey anti-rabbit IgG, anti-goat IgG, and alkaline phosphatase-conjugated donkey anti-mouse IgG were purchased from Jackson Immunoresearch Laboratories (West Grove, PA). DAPT (GSI-IX) was obtained from Selleck Chemicals Biotechnology (Houston, Texas). siGENOME SMARTpools for Notch1 and Notch4 were obtained from Dhamarcon (Thermo Scientific, Waltham, MA). 5-Bromo-4-chloro-3-indoyl phosphate/nitro blue tetrazolium was from Life Technologies (Gaithersburg, MD). Other reagents were obtained from Sigma (St. Louis, MO).

2. Cell culture and establishment of tamoxifen-resistant MCF-7 cells

MCF-7 cells were cultured at 37°C in 5% CO_2/95% air in Dulbecco's modified Eagle's medium (DMEM) containing 10% fetal

bovine serum (FBS), 100units/ml penicillin, and 100μg/ml streptomycin. TAMR-MCF-7 cells were established using the methodology reported previously [35]. Briefly, MCF-7 cells were cultured in phenol-red-free DMEM containing 10% charcoal-stripped, steroid-depleted FBS (C/D FBS) (Hyclone, Logan, UT) and 4-hydroxytamoxifen. The cells were continuously exposed to 4-hydroxytamoxifen and its concentration was gradually increased from 0.1 μM to 3 μM over a 9-month period.

3. Generation of ERα66 overexpressing stable cell line

To generate the stable cell lines with ERα66 over-expression, amphotrophic retroviral supernatants were produced by transfection of the MSCV-GFP or MSCV-GFP-ER66 retro vectors into Phoenix packaging cells. Viral supernatants were harvested 72 h posttransfection, and viral stock was passed through a 0.45 μm filter. For each infection, 3 × 10^4cells of TAMR-MCF-7 or MDA-MB-231 or SKBR3 were plated in six-well culture plates and incubated with viral stocks in a final volume of 2ml (1ml viral supernatant and 1 ml complete media). To enhance the efficiency of infection, 3μg/mL Polybrene was added to the culture media. Remove the virus containing medium every 12 hours and repeat the infection as described above for 20 times. The stable overexpressing-cells were analyzed by immunoblotting for the protein expression.

4. Generation of ERα36 overexpressing stable cell line

MCF-7 cells were plated at a density of $1x10^4$cells/24-well plate overnight, then transfected with an HA-tagged ERα36 expression vector driven by the CMV promoter, an empty expression vector using Lipofectamin 2000 (Invitrogen, Carlsbad, CA). The ERα66 expression vector was provided by Dr. Wang at Creighton University Medical School. Forty-eight hours after transfection, transfected cells were replated and selected with G418 (800 μg/ml)-containing medium for 2 weeks. The medium was changed every three days until colonies appeared. Surviving single colonies were then picked and amplified, named as MCF7-ER36, and used for the experiments. The empty expression vector-transfected MCF-7 cells (MCF7-pcDNA3.1) were used as controls.

5. Generation of ERα36 knockdown stable cell line

To establish cell lines with ERα36 knock-down expression by the shRNA method in TAMR-MCF-7 cells, we odered Sigma to construct an ERα36-specific shRNA expression lentiviral vector. The lentivirus-infected [shLKO (an empty lentiviral vector) or shERα36 constructs]. TAMR-MCF-7 cells were selected in puromycin (5 μg/mL)-containing media for 2 weeks. The expression levels of ERα36 of the puromycin resistant MCF-7 cells were further evaluated by Western blotting. The medium was changed every three days until colonies appeared. Surviving single colonies were then picked and amplified, named as TAMR-shER36, and used for the experiments. The empty expression vector-transfected TAMR-MCF-7 cells (TAMR-shc) were used as controls.

6. siRNA knockdown assay

siGENOME SMARTpools for Notch1 and Notch4 were used to knock-down Notch1 and Notch4 expression in MCF-7 and TAMR-MCF-7 cells. Briefly, cells were grown in six-well dishes, then Notch1 siRNA or Notch4 siRNA were transfected using DharmaFECT-1 transfection reagent (Dharmacon, Waltham, MA) according to the manufacturer's protocol. As a transfection control, cells were transfected with control siRNA (nontarget) from the Dharmacon (Thermo Scientific, Waltham, MA). Whole-cell lysates were prepared and subjected to Western blot analyses. siRNA oligo sequences (Notch4-ICD #1, GCCCAACCCUGCGAUAAUG; Notch4-ICD #2, CAACGUAACCACUGGGAUC) were synthesized by Bioneer (Korea). Nontargeting control was purchased from Bioneer (Korea). siRNAs were transfected into TAMR-MCF-7 cells using Lipofectamine 2000 (Invitrogen, Carlsbad, CA).

7. Preparation of nuclear extracts

Cells were washed with ice-cold PBS. The cells were then scraped, transferred to microtubes, and allowed to swell after adding 100 μl of a hypotonic buffer containing 10 mM HEPES (pH 7.9), 10 mM KCl, 0.1 mM EDTA, 0.5% Nonidet P-40, 1 mM dithiothreitol, and 0.5 mM phenyl methyl sulfonyl fluoride. The lysates were incubated for 10 min on ice and centrifuged at 7,200×g for 5 min at 4°C. Pellets containing the crude nuclei were resuspended in 50 μl of an extraction buffer containing 20 mM HEPES (pH 7.9), 400 mM NaCl, 1 mM EDTA, 10 mM dithiothreitol, and 1 mM phenyl methyl sulfonyl fluoride and incubated for 30 min on ice. The samples were centrifuged at 15,800×g for 10 min to obtain supernatants containing the nuclear fractions. The nuclear fractions were stored at −70°C

until needed.

8. Immunoblot analysis

Cells were lysed in a buffer containing 20 mM TrisHCl (pH 7.5), 1% Triton X-100, 137 mM sodium chloride, 10% glycerol, 2 mM EDTA, 1 mM sodium orthovanadate, 25 mM β-glycerophosphate, 2 mM sodium pyrophosphate, 1 mM phenyl methyl sulfonyl fluoride, and 1 μg/ml leupeptin. The cell lysates were centrifuged at 10,000×g for 10 min to remove debris, and the proteins were fractionated using a 10% separating gel. The fractionated proteins were then transferred electrophoretically to nitrocellulose paper, and the proteins were immunoblotted with specific primary and corresponding peroxidase-conjugated secondary antibodies.

9. Immunoprecipitation

Cells were solubilized in lysis buffer. An equal amount of each protein lysate was incubated with anti-STAT3 antibody overnight at 4°C, followed by incubation with 20 μl of protein G-Sepharose beads for 2 h. The immune complexes were analyzed by Western blot analyses with anti-Notch4 antibody.

10. Measurement of cell proliferation

For Notch4/STAT3 story: Cells were cultured in 10% FBS-containing medium containing with or without Notch inhibitor for the indicated times. Then viable adherent cells were stained with MTT [3-(4,5-dimethylthiazol-2-yl)-2,5-diphenyl-tetrazolium bromide] (2 mg/ml) for 4 h. Media were then removed and the formazan

crystal-stained cells were dissolved in 200 μl dimethylsulfoxide. Absorbance was measured at 540 nm using a microtiter plate reader (Berthold Tech., Bad Wildbad, Germany).

For ERα66/ERα36 story: Cell proliferation assays were carried out using IncuCyteTM (Essen Bioscience, UK) for time-course experiments. Growth curves were built from confluence measurements acquired during round-the-clock kinetic imaging.

For 10%FBS-stimulated cell proliferation: Cells (5000 cells/well) were seeded in a 96-well plate and allowed to adhere for 8 h. Complete medium was added so that the total volume of each well is 200 μl and then incubated in IncuCyte for 72 h.

For estrogen-stimulated cell proliferation: Cells were plated at a density of 5000 cells/well in phenol red-free DMEM containing 10% C/D FBS overnight. The medium then was replaced with phenol red-free medium supplemented with 1% C/D FBS, and 10 nM 17β-estradiol and incubated in IncuCyte for 72h.

For hormone-deprived condition: Cells were plated at a density of 5000 cells/well in phenol red-free DMEM containing 10% C/D FBS overnight. The medium then was replaced with phenol red-free medium supplemented with 10% C/D FBS, 1% penicillin-streptomycin and incubated in IncuCyte for 72h.

11. Reporter gene assay

A dual-luciferase reporter assay system (Promega, Madison, WI) was used to determine the promoter activity. Briefly, the cells were transiently transfected with 1 μg of MMP2-Luc, pNF-κB-Luc or pAP-1-Luc reporter plasmid and 20 ng of phRL-SV40 plasmid (Renilla luciferase expression for normalization) (Promega, Madison,

WI) using Lipofectamine 2000 (Invitrogen, Carlsbad, CA). Both firefly and Renilla luciferase activities in the cell lysates were measured using a luminometer (Tristar LB 941, Berthold Tech., Bad Wildbad, Germany). The relative luciferase activity was calculated by normalizing the promoter-driven firefly luciferase activity to that of *h*Renilla luciferase.

12. Reverse transcription-polymerase chain reaction (RT-PCR)

Total RNA was isolated from cells using Trizol (Invitrogen, Carlsbad, CA), and complementary DNA was synthesized by reverse transcription using an oligo (dT) primer. PCR was performed using the selective primers as described in the following table. The band intensities of the amplified DNAs were compared after visualization on a UV transilluminator.

Table 2. Sequence of primers for RT-PCR

Gene	Forward Primer 5' - 3'	Reverse Primer 5' - 3'
MMP2	GTATTTGATGGCATCGCTCA	CATTCCCTGCAAAGAACACA
Notch1	GCAAGAACGCCGGGACAT	CTCGTTACAGGGGTTGCTGA
Notch4	TCGGACTTGGTCCGTAGACT	TCTGCTCTGGTGGGCATACA
GAPDH	AGCCACATCGCTCAGACAC	GCCCAATACGACCAAATCC

13. Trans-well migration assay

An *in vitro* cell migration assay was performed using a 24-well Trans-well polystyrene membrane with 8 μm size pores (3422; Corning, Cambridge, MA). The lower side of the upper chamber was covered with type I collagen (Sigma-Aldrich, St. Louis, MO). The cells were seeded in the upper chamber of the Trans-well plate and

the lower chamber was filled with 600 μl serum-containing culture media. The cells were incubated at 37ºC (5% CO_2) for18 h and then fixed with methanol, and subsequently stained with hematoxylin for 10 min followed by eosin staining. For Notch inhibitor treatment, cells were maintained with serum-free media in the presence or absence of (DAPT) at indicated concentrations. For gene silencing, cells were transiently transfected with Notch4 siRNA or control siRNA on the day before, then were added onto the upper chambers with serum-free media. The phenotypes of cell migration were determined by quantifying the cells that migrated to the lower side of the transwell membrane with microscopy (× 20 magnification). Twelve visual fields were counted for each transwell membrane, and each sample was assayed in triplicate.

14. Three-dimensional (3D) spheroid invasion assay

$5x10^3$cells were seeded on 2% matrigel-coated in 24-well plates, and media were refreshed every 2 days. Cell forming 3D spherical structure (spheres) was photographed (× 20 magnification) at 2-day intervals for 10 days.

15. Wound healing assay

TAMR-MCF-7 cells were pre-treated with vehicle or DAPT (10 μM) for 24 h. Cells were then seeded and grown to 100% confluence on a 96-well Essen Bioscience Image Lock Plate (Essen Bioscience, Ann Arbor, MI) at 37°C with 5% CO2. Precise wounds were made in each well using a Wound Maker, a tool designed to make a wound

with consistent size. The plate was placed in an IncuCyte incubator, a live-cell imaging system (Essen Bioscience), and images were taken every 4 h intervals. Relative wound density was calculated by IncuCyteTM Chemotaxis Cell Migration Software as the most robust metric to quantify cell migration.

16. Kaplan-Meier analyses for online survival calculation

Kaplan - Meier analysis of breast cancer (kmplot.com/analysis/) was performed as described previously [36].

17. Immunocytochemistry (ICC) and confocal microscopy

Cells were seeded in 10% complete media on coverslips for 24 h. Coverslips were fixed in 4% paraformaldehyde for 10 minutes at room temperature and then washed twice with 1x PBS. Following washes, samples were permeabilized for 10 minutes in 0.1% Triton X-100, then washed with PBS. Samples were blocked with 10% horse serum ((Invitrogen, Carlsbad, CA) for 1 hour at room temperature. Slides were incubated overnight at +4°C with primary antibody. Samples were washed with PBS and incubated with secondary antibody for 1 hour at room temperature. For F-actin staining to visualize the cytoskeleton, samples were incubated with Alexa Fluor 546 phalloidin (Invitrogen) for 30 min. Slides were washed as above and stained with DAPI for 10 minutes at room temperature. Coverslips were mounted stored until imaging in the dark at +4°C. Images were acquired under iRiSTM Digital Cell Imaging

System (Logos Biosystems, Annandale, VA).

18. Immunohistochemistry (IHC)

Eight TAM-responsive and four TAM-resistant cases [37] were estimated. Tissue sections were immunostained with antibodies directed against Notch1 or Notch4. Briefly, the sections were deparaffinized and then incubated overnight with anti-Notch1 antibody or anti-Notch4 antibody at 4°C, followed by HRP-conjugated anti-rabbit IgG for 30 min. The color was developed by 3,3‘-diaminobenzidine solution. Finally, sections were counterstained with hematoxylin, dehydrated, mounted, and observed.

Immunohistochemistry for detection of proliferating cell nuclear antigen (PCNA) was performed with tumors in tumorigenesis test. IHC was performed with rabbit monoclonal antibodies to PCNA (Santa Cruz, CA). IHC results were recorded by light microscopy. The cell nuclei or membrane was stained yellow or brown suggesting the positive signal.

19. Mouse xenografts

Animal experiments were performed in accordance with guidelines of Seoul National University Animal Care and Use Committee. Female five-week-old athymic (nu/nu) BALB/c mice were obtained and housed in an air-conditioned room at a temperature of 22°C to 24°C and a humidity of 37% to 64%, with a 12-hour light/dark cycle. After 1 week of acclimatization, tumor inoculation was performed. Each 1×10^6 cells of MCF-7, TAMR-MCF-7, MCF7-pcDNA3.1, MCF7-ER36, TAMR-GFP, TAMR-ER66 were mixed at a 1:1 ratio with Matrigel

(BD Biosciences) and inoculated subcutaneously into the both sides of flanks of mice. Tumor diameter was measured with caliper twice per week and tumor volumes were estimated using the following formula: tumor volume (cm^3) = (length×$width^2$)×0.5.

All tumors were excised at the same time, when the largest tumor volume neared 2 cm^3. A small piece of each tumor was frozen for DNA extraction and the remainder was fixed in formalin and embedded in paraffin. Hematoxylin ande osin (H&E) stained sections of tumors were compared.

20. Intrasplenic injection model of liver metastases

Intrasplenic injection model of liver metastases were established using the methodology reported previously [38,39]. The central server for the model instruction can be reached at www.jove.com/video/1977/murine-bioluminescent-hepatic-tumour-model.

Briefly, female five-week-old athymic (nu/nu) BALB/c mice were obtained and housed in an air-conditioned room at a temperature of 22°C to 24°C and a humidity of 37% to 64%, with a 12-hour light/dark cycle. After 1 week of acclimatization, tumor inoculation was performed. Mice were anesthetized and opened the abdomen to expose spleen. The spleen was divided into two hemi-spleens by using black silk suture (Ailee Co., Korea). The mice were then inoculated with $1x10^6$ cells diluted in 100 μl PBS into spleen. For Notch4/STAT3 story, one week after inoculation, mice (n=5/group) were assigned to receive subcutaneous injections daily with either vehicle or DAPT (10 mg/kg) for three additional weeks. The mice

were then sacrificed and the liver samples were analyzed by hematoxylin & eosin (H&E) staining method. All animal procedures were approved by the Institutional Animal Care and Use Committee of Seoul National University (Approve #: ILAR 13-01-027).

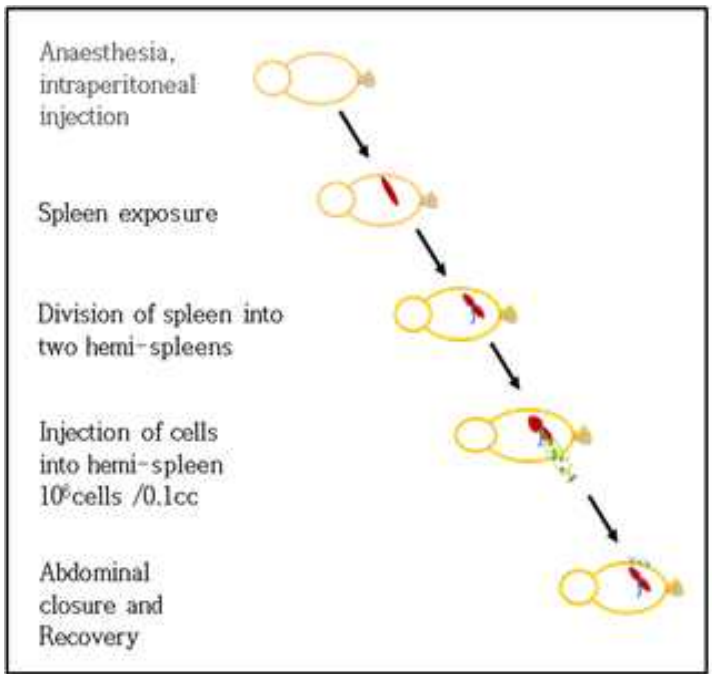

Establishment of hepatic metastases by hemi-spleen injection

21. Data analysis

Student's -test and analysis of variance (ANOVA) test were used to examine the significant intergroup differences. Statistical significance was accepted at either <0.05 or <0.01. A p-value of less than 0.05 was considered statistically significant.

III. RESULTS

Part 1: Role of ERα66/ER36α expression in epithelial-mesenchymal transition of tamoxifen-resistant human breast cancer

1.1. High ERα66 gene expression is associated with better survival in patients with tamoxifen-treated breast cancer

One possible mechanism which could contribute to the development of antiestrogen resistance is the downregulation of ERα66 [18,40]. We analyzed whether the ERα66 gene expression itself was associated with tamoxifen response in a large cohort of ERα66 (+) patients from public data [36]. Kaplan - Meier analysis results showed that ERα66 high expression was statistically correlated with better relapse-free survival (RFS, P=0.04) and distant metastasis-free survival (DMFS, P=0.04) to tamoxifen treatment only (Figs. 1A and 1B).

Several studies revealed that the TAMR-MCF-7 highly expressed ERα36 [18,41,42]. Although statistically not significant, Kaplan - Meier curve analyses displayed that ERα36 high expression tended to be associated with poorer relapse-free survival (RFS, P=0.28) and distant metastasis-free survival (DMFS, P=0.12) to tamoxifen treatment only (Figs. 1C and 1D).

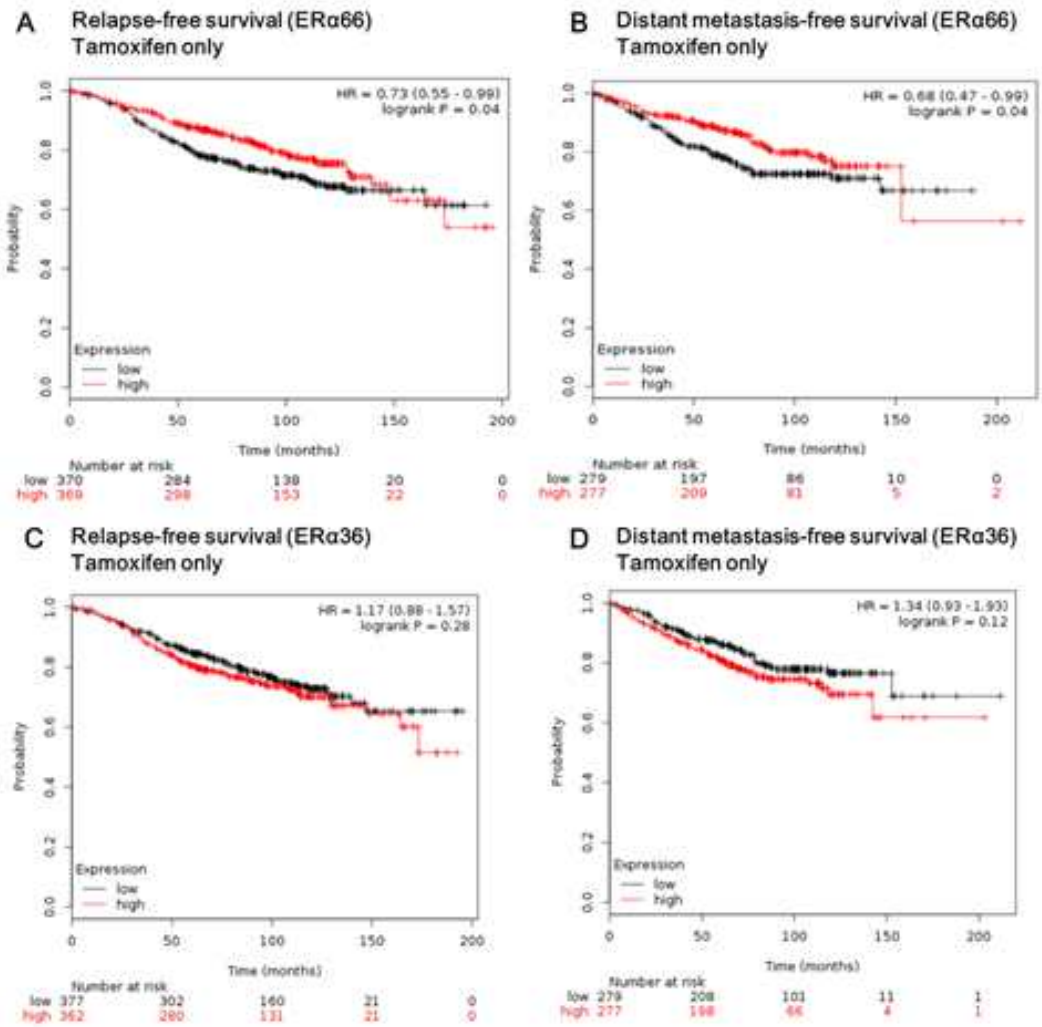

Fig 1. Kaplan-Meier analyses for survival possibility.

(A) Kaplan-Meier analyses for RFS of the cohort of patients with ERα 66-positivity, receiving tamoxifen treatment only without chemotherapy. Affymetrix ID for ERα66 used was 215552_s_at. The cut-off value used in analysis was 316 and the expression range of the probe was 4 - 2922. Patient number for low ERα66 (black) and high ERα66 (red) is presented under the following months.

(B) Kaplan-Meier analyses for DMFS of the cohort of patients with ERα 66-positivity, receiving tamoxifen treatment only without chemotherapy. Affymetrix ID for ERα66 used was 211234_x_at. The cut-off value used in

analysis was 161 and the expression range of the probe was 7 - 3924. Patient number for low ERα66 (black) and high ERα66 (red) is presented under the following months.

(C) Kaplan-Meier analyses for RFS of the cohort of patients with ERα 36-positivity, receiving tamoxifen treatment only without chemotherapy. Affymetrix ID for ERα36 used was 205767_at. The cut-off value used in analysis was 27 and the expression range of the probe was 1 - 8932. Patient number for low ERα36 (black) and high ERα36 (red) is presented under the following months.

(D) Kaplan-Meier analyses for DMFS of the cohort of patients with ERα 36-positivity, receiving tamoxifen treatment only without chemotherapy. Affymetrix ID for ERα36 used was 205767_at. The cut-off value used in analysis was 26 and the expression range of the probe was 1 - 8932. Patient number for low ERα36 (black) and high ERα36 (red) is presented under the following months.

1.2. Expression and localization of ERα66 and ERα36

In order to understand the role of ERα66 and ERα36, we first examined the expression and localization of them in parental MCF-7 and TAMR-MCF-7 cells. We also observed the extreme downregulation of ERα66 and upregulation of ERα36 (Fig. 2A). Then cytosol and nuclear fractionation lysates from these cell lines were analyzed by western blots. The data make clear that ERα36 mainly localized in the cytosol and only small amount fractionates with the nuclei in TAMR-MCF-7 cells (Fig. 2B). ERα66 distributed both in the cytosol and nuclear, but high abundance fractionates with the nuclei in MCF-7 cells (Fig. 2B). Immunofluorescence microscopy was used to identify the subcellular localization of ERα66 and ERα36 in these cell lines. Correspondingly, immunocytochemical staining for ERα66 exhibited strong positive staining in MCF-7 cells but undetected in TAMR-MCF-7 cells and ERα66 is predominantly expressed in nuclear (Fig. 2C). Immunostaining against ERα36 displayed greater staining in TAMR-MCF-7 cells compared to MCF-7 cells (Fig. 2D). These results consistent with previous report that ERα36-expressing HEK-293 cells exhibited 50% of ERα36 fractionates with plasma membrane, 40% with cytosol and 10% with nuclei [16].

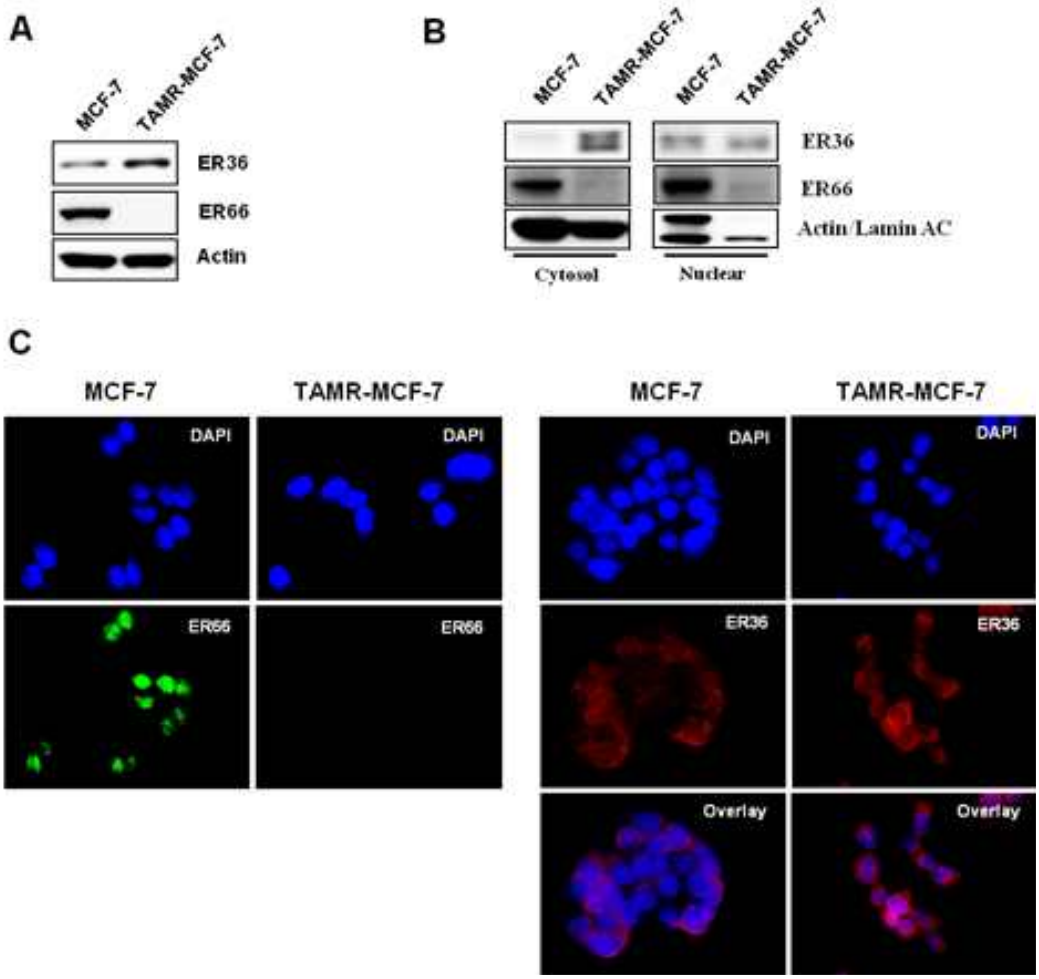

Fig. 2. Expression and localization of ERα66 and ERα36.

(A) Protein expression of ERα66 and ERα36 in MCF-7 and TAMR-MCF-7 cells was determined by immunoblotting.

(B) Expression of ERα66 and ERα36 in the cytosol and nucleus were determined by immunoblotting.

(C) Immunolocalization staining of ERα66 and ERα36 were performed. MCF-7 and TAMR-MCF-7 cells were stained with ERα66 (left) and ERα36 (right) staining in MCF-7 and TAMR-MCF-7 cells. ERα66 was identified with Santa Cruz ERα66 antibody, coupled to secondary anti-mouse IgG tagged with the green fluorescent dye (green). ERα36

was identified with Cell Applications ERα36 antibody, coupled to secondary anti-rabbit IgG tagged with the red fluorescent dye (red). The results are shown as representative images.

1.3. Generation of ERα66 overexpression stable cell line

To further understand the role of ERα66 in tamoxifen-resistant breast cancer, we generate ERα66-overexpressing TAMR-MCF-7 cells. We first used retroviral vector-mediated transduction to stably introduce ERα66 into TAMR-MCF-7 cells. We observed that the expression of ERα66 was greatly increased whereas ERα36 levels did not show significant difference after infection (Fig. 3A). However, immunoblots analyzed cytosol and nuclear fraction from these two cells displayed slightly decrease of ERα36 expression in nuclear (Fig. 3B). The result implies that ERα66 may suppress ERα36 from nuclear translocalization.

Under normal conditions, ERs bind to estrogen, then transfer to the nucleus, subsequently binding to specific EREs and regulating transcription of downstream targets [43]. Other than the traditional genomic pathway, ERs mediate the non-genomic pathway by membrane-associated receptors, results in regulating cellular growth, survival, motility, invasion [44 - 47]. We compared cell proliferation of the ERα66-expressing and parental cells TAMR-MCF-7 cells. As shown in Fig. 3C, overexpression of ERα66 in TAMR-MCF-7 cells did not affect cell growth ability in normal estrogen-deprived condition. Previous reported have demonstrated that ERα36 is a potent mediator of membrane-initiated signaling pathways [16,48]. In ERα66-overexpressing TAMR-MCF-7 cell, ERα36 expression did not show any significant difference compared to control cells in both cytosol and total fractionation (Figs. 3A and 3B). We next examined the effect of ERα66 overexpression on membrane-initiated signaling

pathways, such as MAPK/ERK, PI3K/AKT, and Src pathways. As we seen in Fig. 3D, ERα66 expression did not impact in these growth factor signaling.

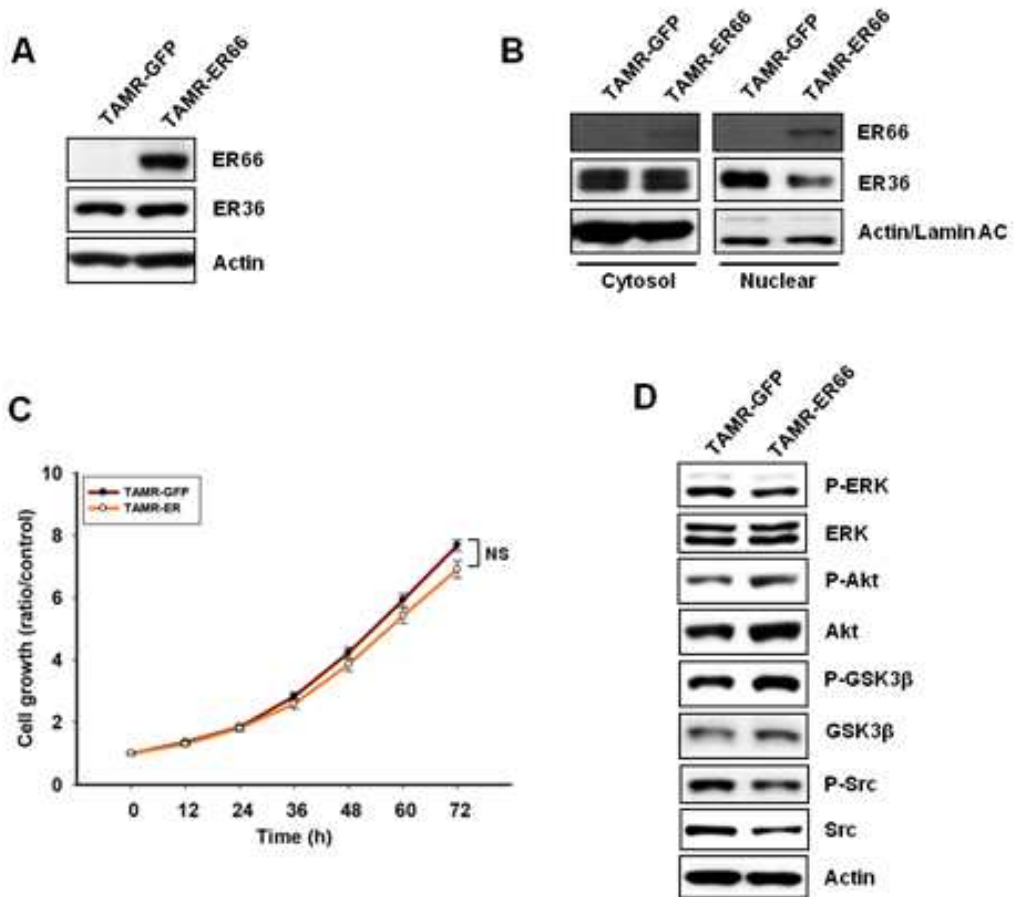

Fig. 3. Overexpression of ERα66 did not affect on cell growth and growth factor signaling.

(A) Establishment of stable TAMR-MCF-7 cells overexpressing either GFP vector (TAMR-GFP) or GFP-ERα66 (TAMR-ER66). Levels of ERα66 and ERα36 in ERα66-overexpressing TAMR-MCF-7 and control cells were determined by immunoblotting.

(B) Expression of ERα66 and ERα36 in the cytosol and nucleus were determined by immunoblotting.

(C) Cell proliferation was measured at different time points using IncuCyte™

(Essen Bioscience, UK) as described in Material and methods. Data represent mean ± SD with 6 different samples.

(D) Overexpression of ERα66 in TAMR-MCF-7 cell does not affect growth factors signaling.

1.4. ERα66-overexpressing TAMR-MCF-7 cells expressed comparable tumorigenesis capacity with control cell

In order to test the role of ERα66 in tumorigenesis capacity, xenograft experiment was performed. TAMR-GFP cells were transplanted into the left sides of nude mice whereas TAMR-ER66 cells were transplanted into the right sides of nude mice (Fig. 4A). Tumors formation in TAMR-ER66-implanted groups displayed comparable enlargement with tumors in TAMR-GFP-transplanted groups (Fig. 4B)

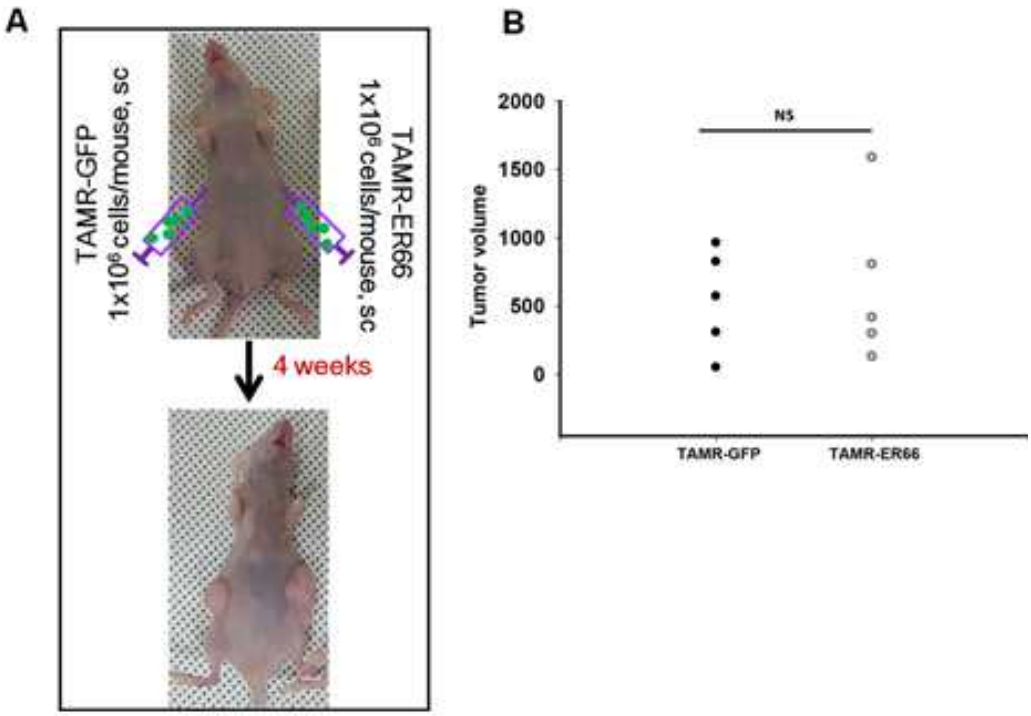

Fig. 4. In xenograft model, mice-bearing TAMR-GFP cells and TAMR-ER66 cells exhibited comparable tumorigenicity.

(A) A representative photo of tumors from nude mice 28 days post-injection of TAMR-GFP cells (left side) and TAMR-ER66 cells (right side) which

the tumors were similarly enlarged on both left and right sides.
(B) Tumor volumes of mice xenografts with TAMR-ER66 cells were no significant difference as compared to the control TAMR-GFP cells at day 28.

1.5. Overexpression of ERα66 suppressed the EMT and migratory capacity of TAMR-MCF-7 cells

Bouris et al. reavealed that silencing of endogenous ERα66 in MCF-7 cells resulted in potent induction of the EMT program [49]. It is consistent with our data that TAMR-MCF7 have typical EMT phenotype and high capacity of migration and metastasis. Here, we examined the role of ERα66 expression in EMT phenotype of tamoxifen-resistant breast cancer. Interestingly, overexpression of ERα66 reversed the EMT to mesenchymal-epithelial transition (MET) characterized by rescue of E-cadherin expression and downregulation of mesenchymal marker such as Snail and Vimentin (Fig. 5A). Immunofluorescence analysis of E-cadherin and F-actin displayed upregulated expression of E-cadherin and reduced cytoskeleton polarization in ERα66-overexpressing TAMR-MCF-7 (Fig. 5B). Trans-well migration assay showed that TAMR-ER66 cells possess weaker in vitro migratory ability than the control TAMR-GFP cells (Fig. 5C). These results imply that ERα66 plays a critical role for EMT program in tamoxifen-resistant breast cancer.

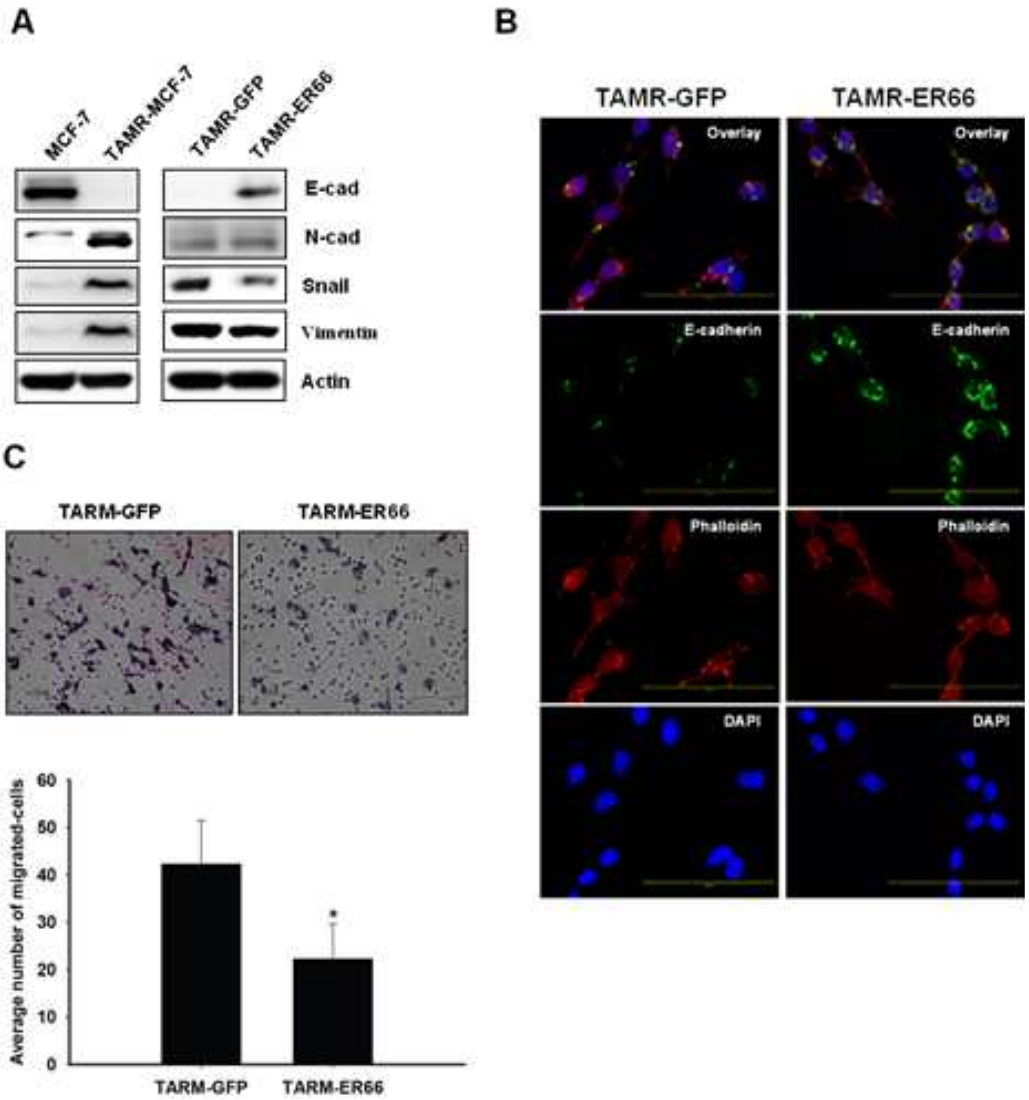

Fig. 5. ERα66-overexpressing TAMR-MCF-7 (TAMR-ER66) cells displayed the inhibitory effect of migratory capacity.

(A) Immunoblot analyses of EMT markers in parental MCF-7 cells, TAMR-MCF-7 cells, TAMR-GFP cells and TAMR-ER66 cells.

(B) Immunofluorescence staining of cell - cell junction protein E-cadherin and the actin cytoskeleton. TAMR-GFP and TAMR-ER66 cells were stained with E-cadherin (green), Phalloidin (red) as well as DAPI (blue) and pictures were taken at × 40 magnification. The results are shown as representative images from three biological replicate experiments.

(C) Trans-well migration assays demonstrating the reduction on migratory ability of ERα66-overexpressing TAMR-MCF-7 cells compared to control cells. Representative microscopy (×20) images of TAMR-GFP and TAMR-ER66 cells (upper). The average migration cell number per field among different experimental groups (lower). Data represent the mean ± SD of three replicates ($^{*}p<0.05$, significant difference versus TAMR-GFP).

1.6. Overexpression of ERα66 resulted in EMT inhibition but not enough for metastasis suppression

Next, we investigated whether suppression of EMT impacts metastasis. An intrasplenic injection model of liver metastases was performed. Mice were implanted with TAMR-GFP cells or TAMR-ER66 cells into hemi-spleen. There was no obvious difference in tumor formation in spleens and susceptibility to macroscopic metastases on the liver surfaces of mice bearing TAMR-GFP cells and mice bearing TAMR-ER66 cells (Figs. 6A-C). These results denoted that ERα66 overexpressing markedly inhibited EMT and cell migration in vitro but had no effect on metastasis suppression in vivo.

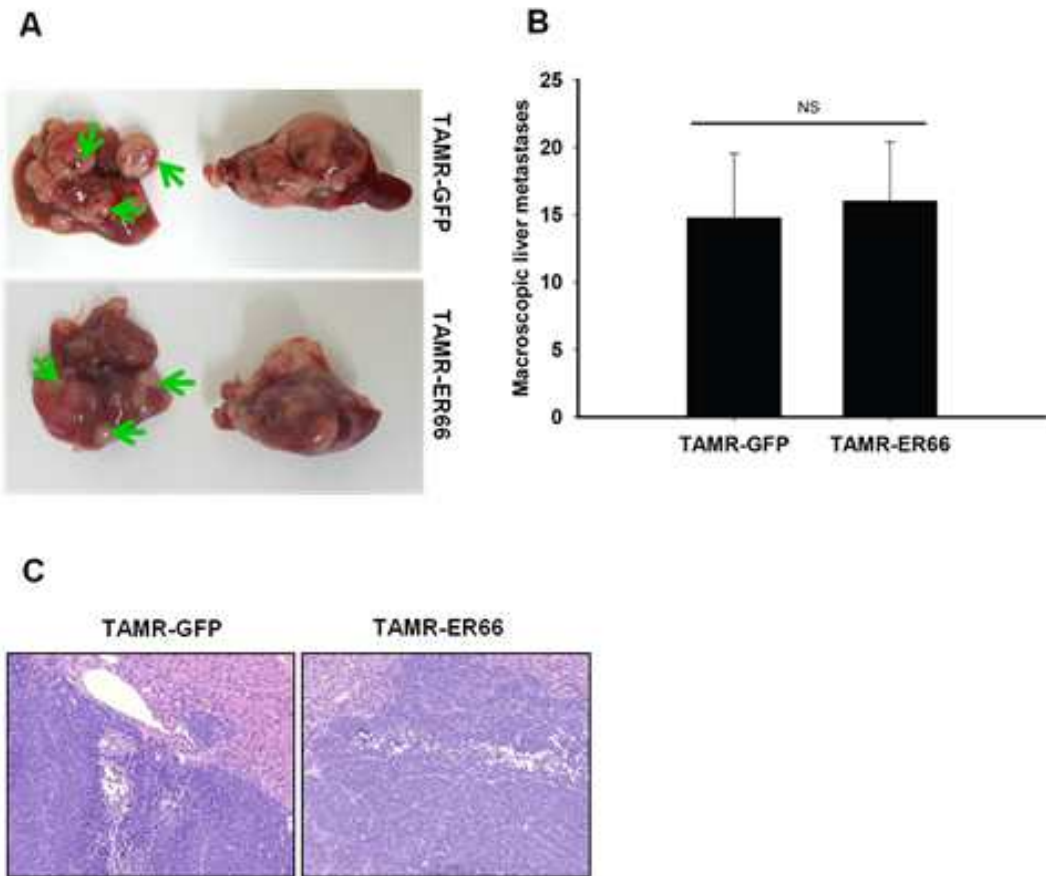

Fig. 6. TAMR-ER66 cells displayed no obvious difference in metastatic tumor burden compared with control cells in model of liver metastases

(A) Representative macroscopic liver metastases. Green arrow indicates macroscopic metastases identified on the surface of livers.

(B) Numbers of macroscopic liver metastases were counted in mice bearing control TAMR-GFP cells and TAMR-ER66 cells. Data represents mean ± SD (n=5).

(C) Representative images of H&E-stained liver sections from each group.

1.7. Establishment of ERα36-overexpressing MCF-7 cells

In order to examine the role of ERα36, we upregulated the expression of ERα36 in MCF-7 cells via stable transfection. As shown in Figs. 7A and 7B, control MCF7-pcDNA3.1 cells expressed very low level of endogenous ERα36 and high expression of endogenous ERα66 whereas cells ERα36-overexpressing MCF-7 (MCF7-ER36) possessed significantly increased level of ERα36 and displayed nearly undetectable ERα66 expression. We found that ERα36 inhibits the transcriptional transactivation activities mediated by the AF-1 and AF-2 domains of ERα66. ERE-luciferase assay exhibited a significant increase in ERα transcriptional activity by estrogen stimulation in MCF-7 but no significant difference in ERα transcriptional activity with ERα36-overexpressing MCF-7 cells (Fig. 7C). Surprisingly, ERα36 overexpressing in MCF-7 cells strongly induced cellular phenotypic changes. Phase contrast microscopy images of parental MCF-7 and control MCF-7-pcDNA3.1 cells showed a typically epithelial morphology, whereas TAMR-MCF-7 cells and ERα36-overexpressing MCF-7 cells exhibited change in morphology to a spread, spindly morphology characteristics of mesenchymal cells (Fig. 7D).

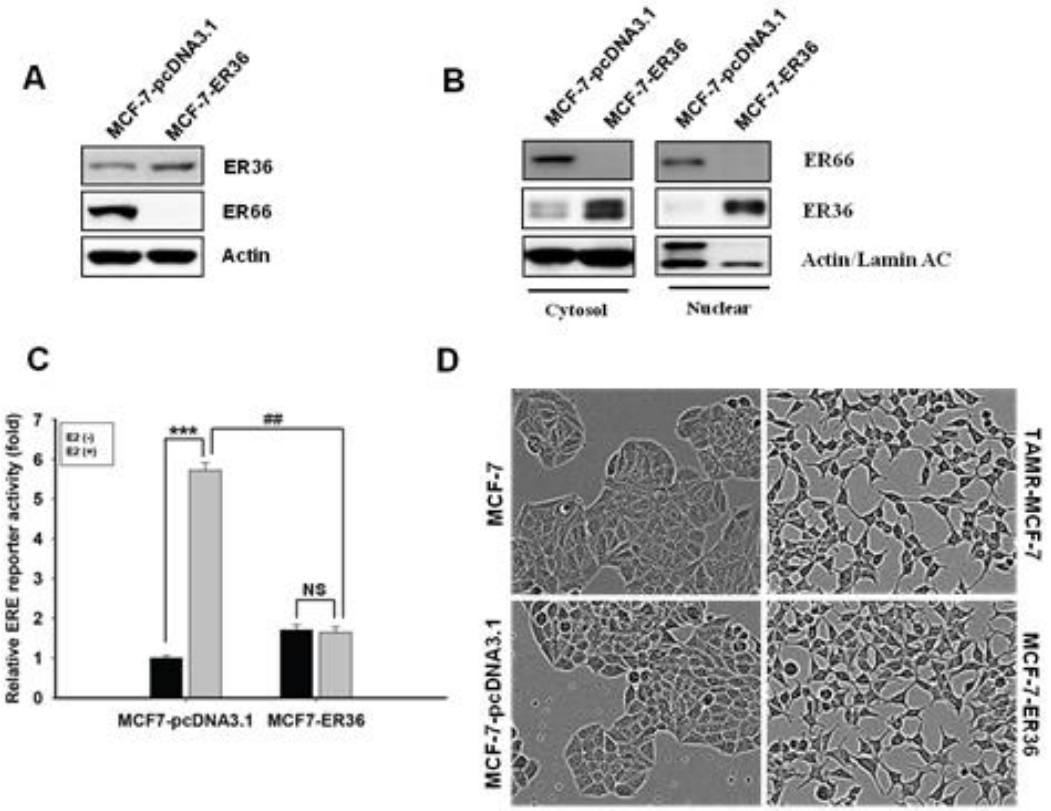

Fig. 7. Establishment of ERα36-overexpressing MCF-7 cells.

(A) Levels of ERα66 and ERα36 in ERα36-overexpressing MCF-7 (MCF7-ER36) and control (MCF7-pcDNA3.1) cells were determined by immunoblotting.

(B) Expression of ERα66 and ERα36 in the cytosol and nucleus were determined by immunoblotting.

(C) ERα36 inhibits the transcriptional transactivation activities mediated by the AF-1 and AF-2 domains of ERα66. Cells were transiently transfected with ERE-luc reporter (1 μg/ml) and phRL-SV (hRenilla) (1 ng/ml) plasmids. Cells were then treated with or without 17β-estradiol (E2; 10 nM) for 18 h before being assayed for luciferase activity. Luciferase assays were performed by using the luciferase assay kit from Promega. Reporter gene activity was calculated as a relative ratio of firefly luciferase to hRenilla luciferase activity. Data represent mean ± SD of 4 seperate samples ($^{***}p<0.001$ significant as compared to MCF7-pcDNA3.1 cells; $^{\#\#}p<0.01$,

significant as compared to estrogen-stimulated MCF7-pcDNA3.1 cells; control level = 1).

(D) ERα36 overexpressing-MCF-7 cells display the mesenchymal morphology. Representative figure of morphological characteristics of MCF-7 cells, TAMR-MCF-7 cells, MCF7-pcDNA3.1 cells and MCF7-ER36 cells in vitro culturing.

1.8. Overexpression of ERα36 activates growth factors and stimulates estrogen-independent cell proliferation

Furthermore, we observed MCF7-ER36 cells proliferated much more rapidly than control MCF7-pcDNA3.1 cells in both 10% FBS-stimulated condition and estrogen-deprived condition (Figs. 8A and 8C). TAMR-MCF-7 cells also displayed accelerated proliferation rate compared to control MCF-7 cells in complete medium (Fig. 8A), however, cell growth was markedly inhibited by 17β-estradiol (Fig. 8B). In the presence of 17β-estradiol, MCF7-ER36 cells did not show any significant difference in growth rate compared to control MCF7-pcDNA3.1 cells (Fig. 8B). These results suggested that there may have other stimulations to the growth of MCF7-ER36 cells except estrogen. We next examined the effect of ERα36 overexpression on membrane-initiated signaling pathways, such as MAPK/ERK, PI3K/Akt, and Src pathways. Interestingly, both MCF7-ER36 and TAMR-MCF-7 exhibited greatly upregulation of these signaling pathways compared to control cells. (Figure 8D). Our data thus demonstrated that ERα36 expression stimulates estrogen-independent cell proliferation.

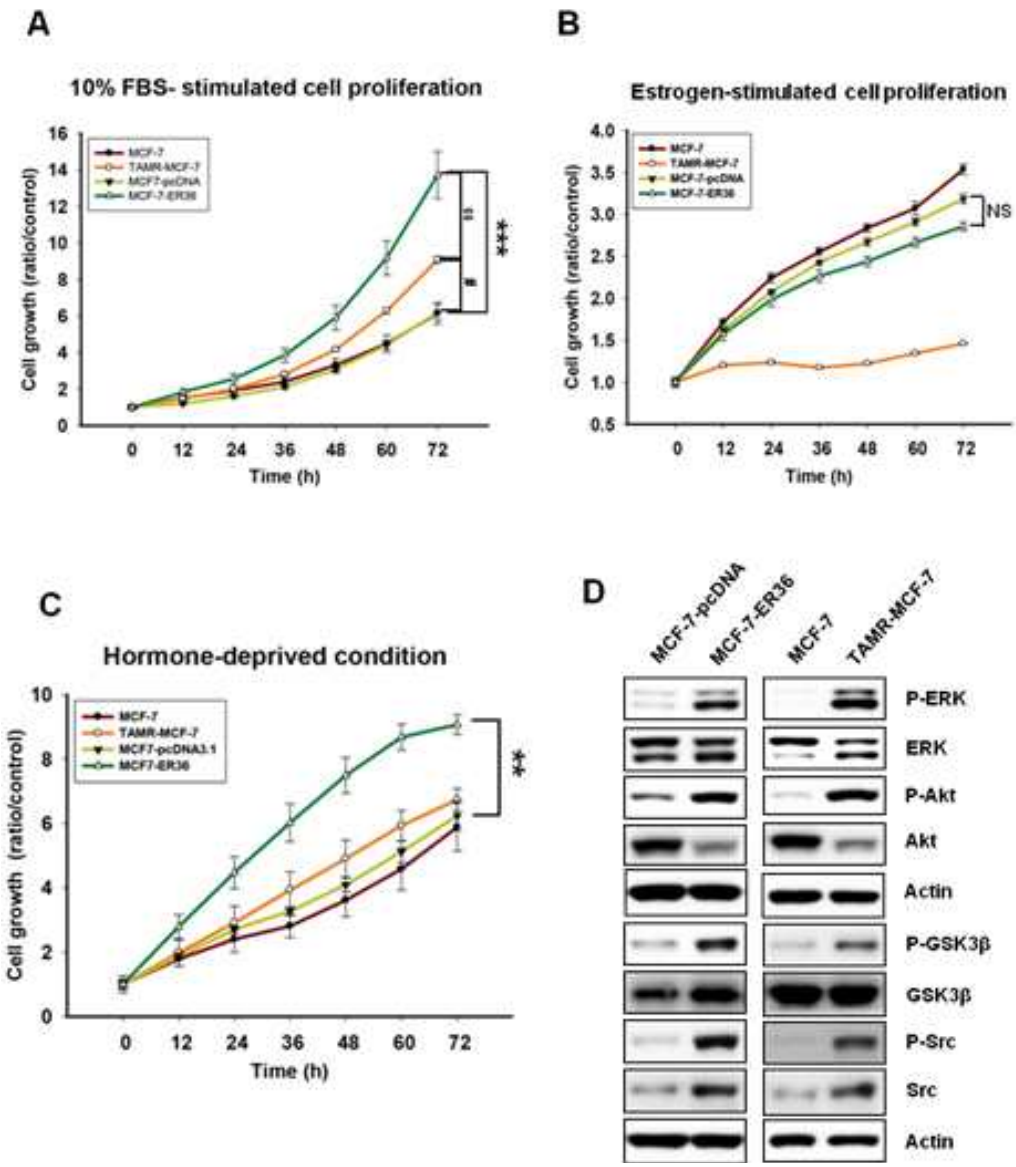

Fig. 8. Overexpression of ER36 activates growth factors and stimulates estrogen-independent cell proliferation.

(A) Relative cell proliferation rate of parental MCF-7 cells, TAMR-MCF-7 cells, MCF7-pcDNA3.1 cells and MCF7-ER36 cells stimulated by 10%FBS were determined at different time points using IncuCyte (Essen Bioscience, UK). Data represent mean ± SD with 6 different samples ($^{\#}p<0.05$, significant difference versus MCF-7, $^{***}p<0.001$, significant difference versus

MCF7-pcDNA3.1, $^{\$\$}p<0.05$, significant difference versus TAMR-MCF-7).

(B) Relative cell proliferation rate of parental MCF-7 cells, TAMR-MCF-7 cells, MCF7-pcDNA3.1 cells and MCF7-ER36 cells stimulated by 17β-estradiol were determined at different time points using IncuCyte (Essen Bioscience, UK). Data represent mean ± SD with 6 different samples.

(C) Relative cell proliferation rate of parental MCF-7 cells, TAMR-MCF-7 cells, MCF7-pcDNA3.1, MCF7-ER36 were further determined at different time points using IncuCyte (Essen Bioscience, UK) after depleting estrogen from the medium as describe in materials and methods.

(D) Overexpression of ERα36 tended to promote estrogen-independent cell proliferation through growth factor signaling stimulation. Immunoblots displayed expression of ERK, Akt, GSK3β, Src and their phosphorylation in parental MCF-7 cells, TAMR-MCF-7 cells, MCF7-pcDNA3.1 cells and MCF7-ER36 cells.

1.9. ERα36-overexpressing MCF-7 cells displayed aggressive tumorigencity in tumorigenesis test

Next, we generated xenograft model to examine the tumorigenesis capacity of ERα36 overexpressing-MCF-7 cells. Female six-week-old BALB/c mice were divided into two groups: mice bearing parental MCF-7 cells and TAMR-MCF-7 cells (group 1), mice bearing control MCF7-pcDNA3.1 cells and ER36-overexpressing MCF7 cells (group 2). Cells were subcutaneously implanted into the left and right sides of nude mice as shown in Fig. 9A. Compared with the control, ERα36 overexpression resulted in rapid tumor growth in mice that had to be killed before the control reached comparable sizes of tumors (Fig. 9A). Similar results was observed in group 1, TAMR-MCF-7 cells exhibited aggressive tumor formation whereas MCF-7 cells did not show that ability (Fig. 9A). Tumors formation from MCF7-ER36 cells displayed comparable enlargement with tumors from TAMR-MCF-7 cells (Figs. 9B and 9C).

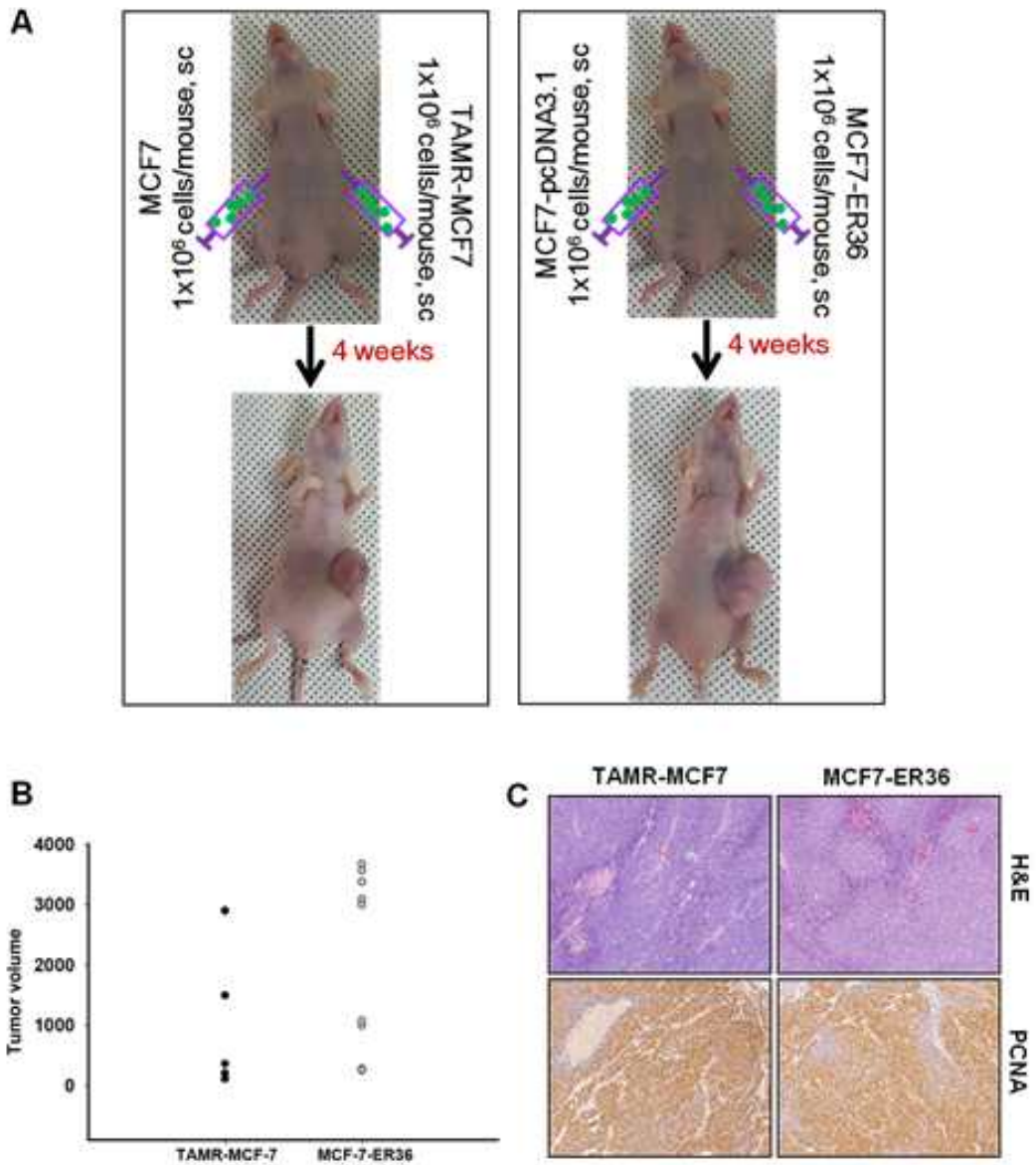

Fig. 9. ERα36 overexpressing-MCF-7 cells displayed aggressive tumorigencity in tumorigenesis test.

(A) Left panel, representative photos of tumors from nude mice 28 days post-injection of MCF-7 cells (left side) and TAMR-MCF-7 cells (right side)). Right panel, representative photos of tumors from nude mice 28 days post-injection of MCF7-pcDNA3.1 cells (left side) and MCF7-ER36 cells (right side).

(B) Tumor volumes of mice xenografts with MCF7-ER36 cells exhibits more aggressive tumorigencity compared to the TAMR-MCF-7 cells at day 28.
(C) Representative histopathological images of tumor mass were examined by H&E staining (upper). Immunohistochemical images of representative tumor tissues stained with PCNA antibody, marker of proliferative cells (lower). The cell nuclei or membrane was stained brown suggesting the positive signal.

1.10. ERα36-overexpressing MCF-7 cells exhibited typical morphological EMT feature and enhanced in vitro migratory ability

We have demonstrated that ERα36 overexpression in MCF-7 cells strongly induced cellular phenotypic changes (Fig. 7D). In order to assess any morphological changes, cells were stained with Rhodamine-phalloidin and co-stained for E-cadherin. Phalloidin staining reveals actin filaments which regulated cell migration was reorganized in MCF7-ER36 cells and TAMR-MCF-7 cells (Fig. 10B). E-cadherin is predominantly localized at cell-cell contacts in epithelial cells such as MCF-7 cells and MCF7-pcDNA3.1 cells, while staining intensive was reduced in MCF7-ER36 cells and TAMR-MCF-7 cells (Fig. 10B). Data from Western blots analyses confirmed these results. As seen in Fig. 10A, expression of several markers typical of EMT such as N-cadherin, Snail, Vimentin were markedly upregulated, whereas E-cadherin expression was extremely downregulated. Trans-well migration assay showed that MCF7-ER36 cells possess much greater in vitro migratory ability than the control MCF7-pcDNA3.1 cells (Fig. 10C). These results imply that ERα36 expression seems to be involved in EMT program in breast cancer cells.

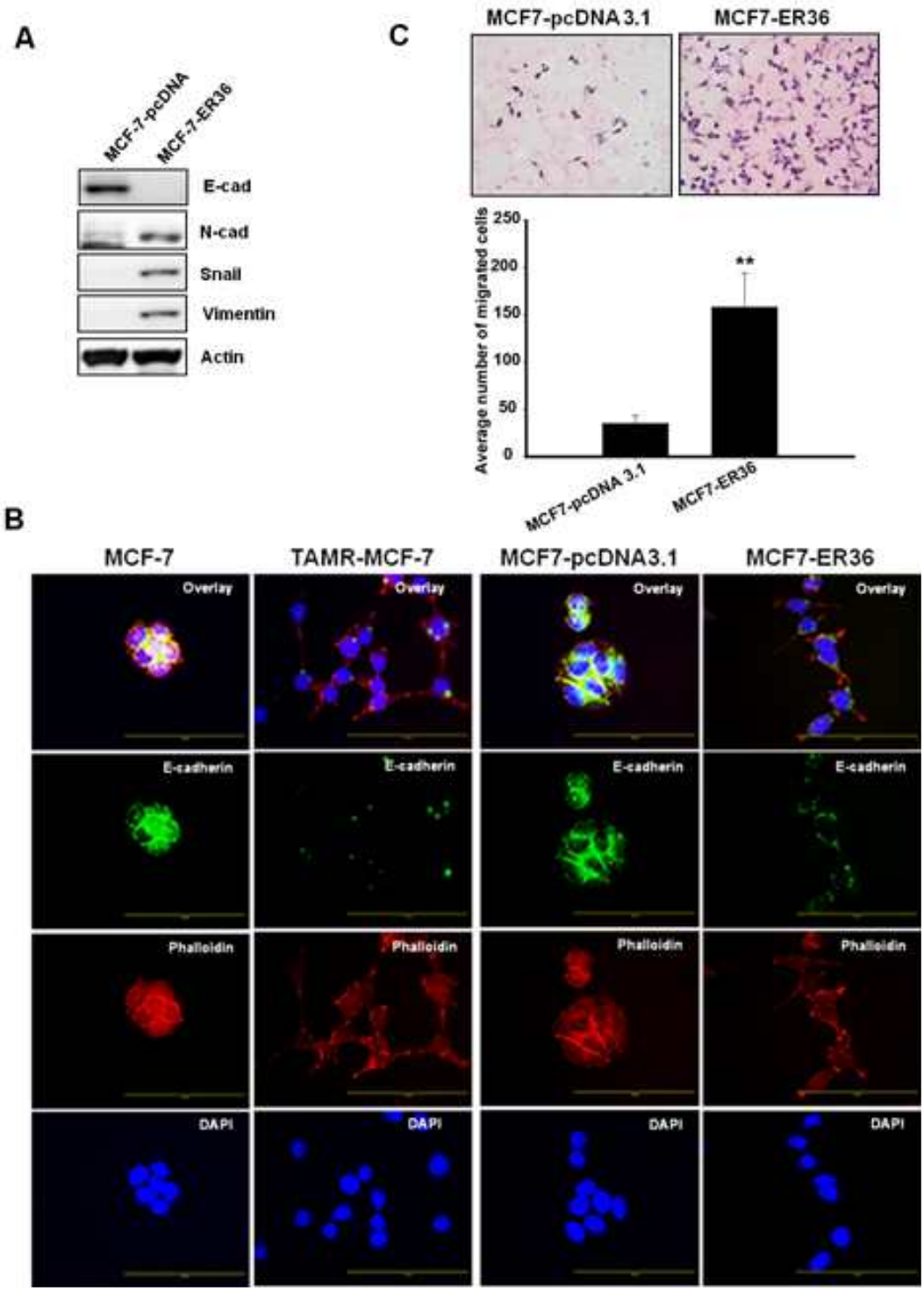

Fig. 10. Overexpression ERα36 in MCF-7 cells induces EMT phenotype changes.

(A) Immunoblot analyses of EMT markers in parental MCF-7 cells, TAMR-MCF-7 cells, MCF7-pcDNA3.1 cells and MCF7-ER36 cells.
(B) Immunofluorescence staining of cell - cell junction protein E-cadherin and the actin cytoskeleton. MCF-7 cells, TAMR-MCF-7 cells, MCF7-pcDNA3.1 cells and MCF7-ER36 cells were stained with E-cadherin (green), Phalloidin (red) as well as DAPI (blue) and pictures were taken at × 40 magnification. The results are shown as representative images from three biological replicate experiments.
(C) Trans-well migration assays demonstrating the increase on migratory ability of ERα36-overexpressing MCF-7 cells compared to control cells. Representative microscopy (× 20) images of MCF7-pcDNA3.1 cells and MCF7-ER36 cells (upper). The aver
age migration cell number per field among different experimental groups (lower). Data represent the mean ± SD of three replicates ($^{**}p<0.01$, significant difference versus MCF7-pcDNA3.1).

1.11. ERα36-overexpressing MCF-7 cells possessed high capacity of tumorigenesis but not metastasis

Overexpression of ERα36 in MCF-7 cells resulted in a potent EMT and enhanced migration and estrogen-independent cell proliferation. Notably, these cells exhibited similar characteristics to TAMR-MCF-7 cells. We then performed intrasplenic injection model of liver metastases. Mice were implanted with MCF-7 cells, TAMR-MCF-7 cells, MCF7-pcDNA3.1 cells or MCF7-ER36 cells into hemi-spleens. No tumor formation or metastases were observed in mice bearing MCF-7 cells or MCF7-pcDNA3.1 cells (Fig. 11). On the contrary, mice implanted with TAMR-MCF-7 cells exhibited strongly susceptibility to both tumorigenesis and metastases (Fig. 11). Metastasis did not occur despite MCF7-ER36 cells caused aggressive tumor formation in spleen (Fig. 11). These results denoted that ERα36 is involved in EMT process but not a sole factor for metastasis of TAMR-MCF-7 cells.

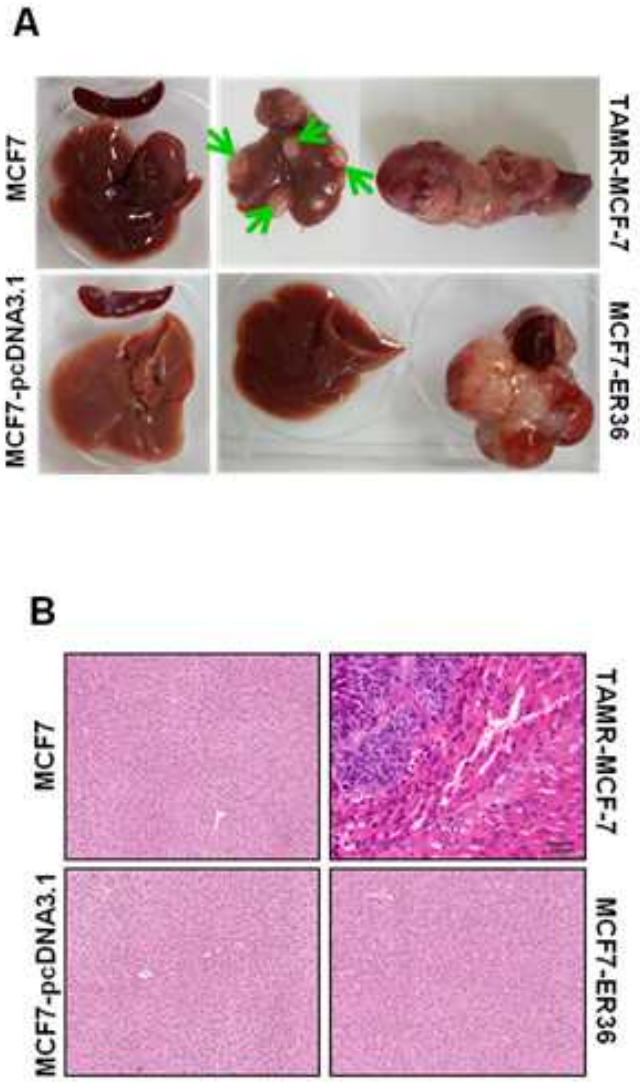

Fig. 11. ERα36 is involved in EMT process but not a sole factor for metastasis of TAMR-MCF-7 cells.

(A) Representative photos of livers from nude mice 5 weeks post-injection of either MCF-7 cells, TAMR-MCF-7 cells, MCF7-pcDNA3.1 cells or MCF7-ER36 cells into hemi-spleens. Green arrow denotes macroscopic metastases identified on the surface of livers.

(B) Representative images of H&E-stained liver sections from each group.

1.12. Generation of ERα36 knockdown stable cell line

We further knocked down ERα36 expression in TAMR-MCF-7 cells using lentivirus system. Western blotting analysis confirmed the significantly decreased expression of endogenous ERα36 in cells transfected with ERα36 shRNA (Fig. 12A). ERα36 silencing in TAMR-MCF-7 cells (TAMR-ER36sh) exhibited decreased cell proliferation rate compared to control cells (TAMR-shc) in hormone-deprived condition (Fig. 12B). Next, we investigated the expression of membrane-initiated signaling pathways, such as MAPK/ERK, PI3K/Akt, and Src in ERα36 silencing TAMR-MCF-7 cells. As shown in Fig. 12C, ERK and PI3K/Akt signaling were suppressed by ERα36 knockdown in TAMR-MCF-7 cells. The result is consistent with previous report that MAPK/ERK and PI3K/Akt signaling pathways are mediated by ERα36 induce the expression of protooncogene c-Myc, which has profound mitogenic effects [16,50]. We further examined effect of ERK inhibitor (PD98059; 30 μM) or PI3K inhibitor (LY294002; 30 μM) on cell growth of TAMR-MCF-7 cells. Fig. 12D showed that cell proliferation rate was significantly reduced in the presence of these inhibitors. Our data thus demonstrated that ERα36 knockdown suppressed estrogen-independent cell proliferation of TAMR-MCF-7 cells via MAPK/ERK and PI3K/Akt pathways.

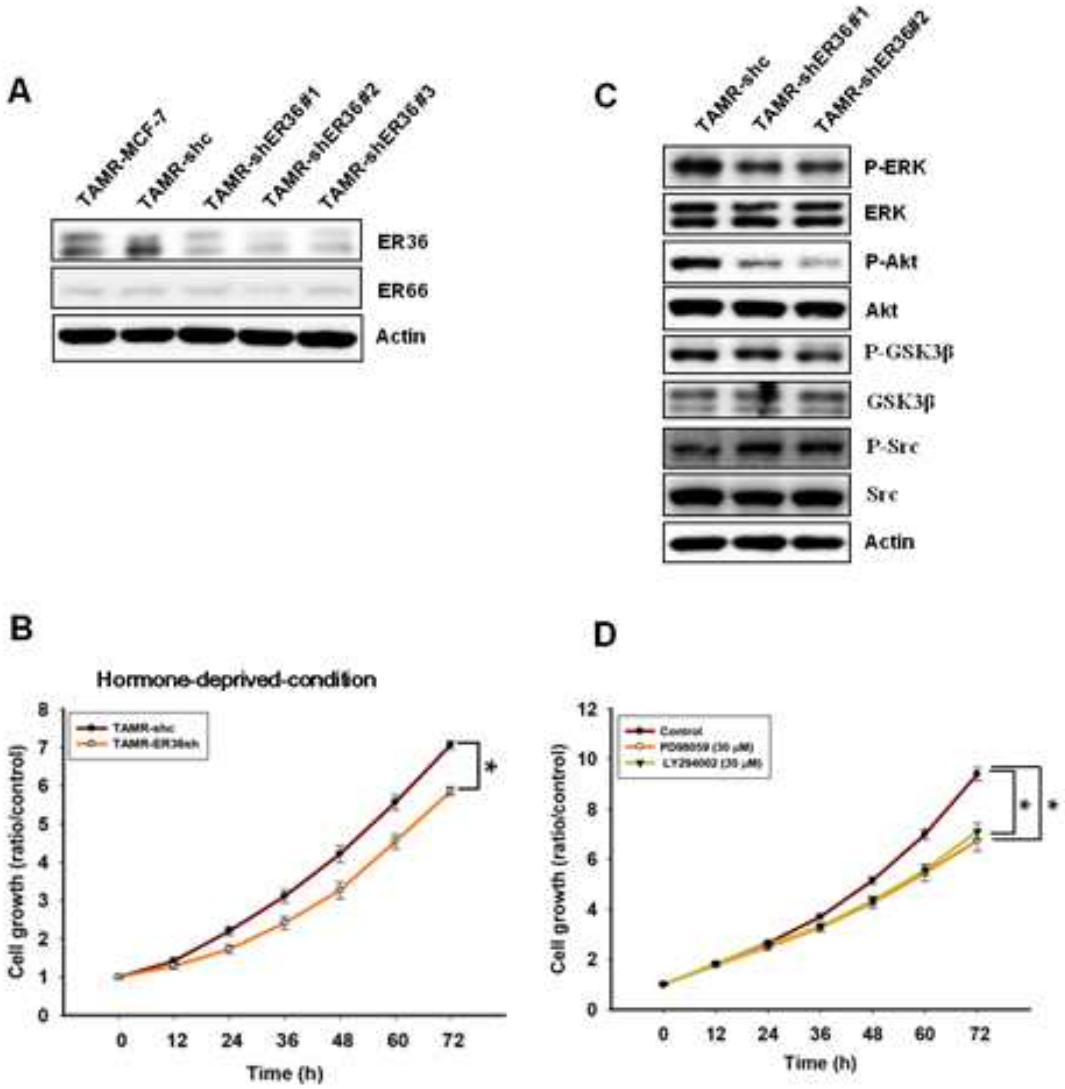

Fig. 12. ER36 knockdown suppresses estrogen-independent cell proliferation of TAMR-MCF-7 cells via ERK and PI3K/Akt pathways.

(A) Establishment of ER36 knock-out in TAMR-MCF-7 cells. Protein expression of ERα66 and ERα36 in ERα36-silencing TAMR-MCF-7 cells (TAMR-shER36) and control cells (TAMR-shc) cells were determined by immunoblotting.

(B) Relative cell proliferation rate of parental TAMR-shc cells, TAMR-shER36 cells determined at different time points using IncuCyte

(Essen Bioscience, UK) after depleting estrogen from the medium as describe in materials and methods. Data represent mean ± SD with 6 different samples ($^{*}p<0.05$, significant difference versus TAMR-shc).

(C) Immunoblots displayed expression of ERK, Akt, GSK3β, Src and their phosphorylation in TAMR-shc cells and TAMR-shER36 cells.

(D) Relative cell proliferation rate of TAMR-shER36 cells treated with either vehicle, LY294002 (30 μM) or PD98059 (30 μM) determined at different time points using IncuCyte (Essen Bioscience, UK). Data represent mean ± SD with 6 different samples ($^{*}p<0.05$, significant difference versus control).

1.13. Silencing of ER36 did not affect on EMT and migratory capacity of TAMR-MCF-7 cells

ERα36 overexpressing in MCF-7 cells markedy induced cellular phenotypic changes accompanied by downregulation of epithelial molecule E-cadherin expression and greatly elevation of several mesenchymal protein markers. However, ERα36 knockdown did not impact any significant change in EMT markers (Fig. 13A) as well as migratory capacity (Fig. 13B) of TAMR-MCF-7 cells. These results denote that ERα36 overexpression evokes downregulation of ERα66 in ERα66-positive breast cancer cells, which is involved in EMT-mediated cell migration. However, ERα36 is not sole factor for EMT progression.

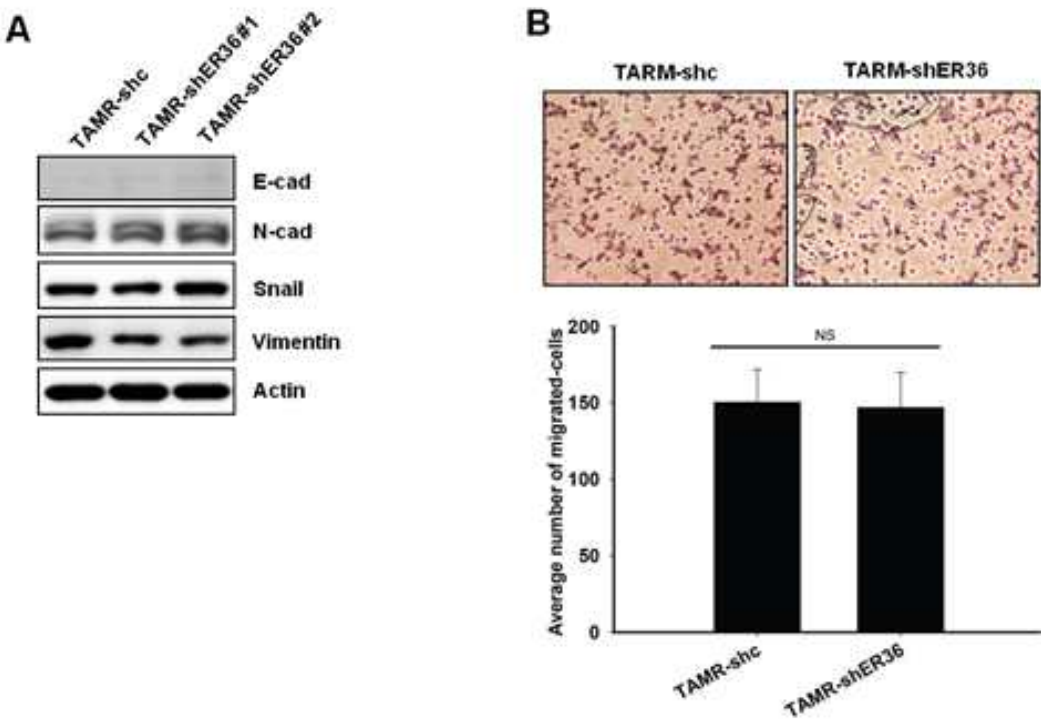

Fig. 13. Knockdown of ERα36 did not impact on EMT and migratory

capacity of TAMR-MCF-7 cells.

(A) Immunoblot analyses of EMT markers in control TAMR-shc cells and TAMR-shER36 cells.

(B) Trans-well migration assays exhibited no significant difference between ERα36-silencing TAMR-MCF-7 cells and control cells. Representative microscopy (× 20) images of TAMR-shc and TAMR-ERsh36 cells (upper). The average migration cell number per field among different experimental groups (lower). Data represent the mean ± SD of three replicates.

1.14. Upregulation of ERα66 in ERα66-negative breast cancer cells suppresses EMT and migratory ability in vitro

Several reports revealed that the loss of estrogen receptor ERα66 induced epithelial EMT in human breast cancer cells [49,51]. Our data clearly demonstrated that overexpression of ERα66 suppressed EMT-mediated cell migration. We further generated ERα66 overexpressing in other ERα66-negative cell types using retrovirus system. First, we overexpressed ERα66 in MDA-MB-231 cells which possessed mesenchymal properties and high capacity of migration and metastasis (Fig. 14A). Upregulation of ERα66 in MDA-MB-231 cells strongly inhibited EMT phenotype characterized by the elevation of E-cadherin expression and downregulation of mesenchymal markers N-cadherin, Snail, Vimentin (Fig. 14A). Notably, ERα66 overexpressing MDA-MB-231 cells exhibited remarkably reduction of cell migration compared to control cells (Fig. 14B). We then performed ERα66 overexpression in SKBR3 cells which display an epithelial morphology in tissue culture (Fig. 14C). ERα66 overexpressing SKBR3 cells did not show the rescue of E-cadherin expression, however, these cells still displayed the suppression of N-cadherin and Slug levels (Fig. 14C) as well as the reduction of cell migration (Fig. 14D). Our study thus indicated that ERα66 plays a critical role in maintenance of epithelial properties in breast cancer cells.

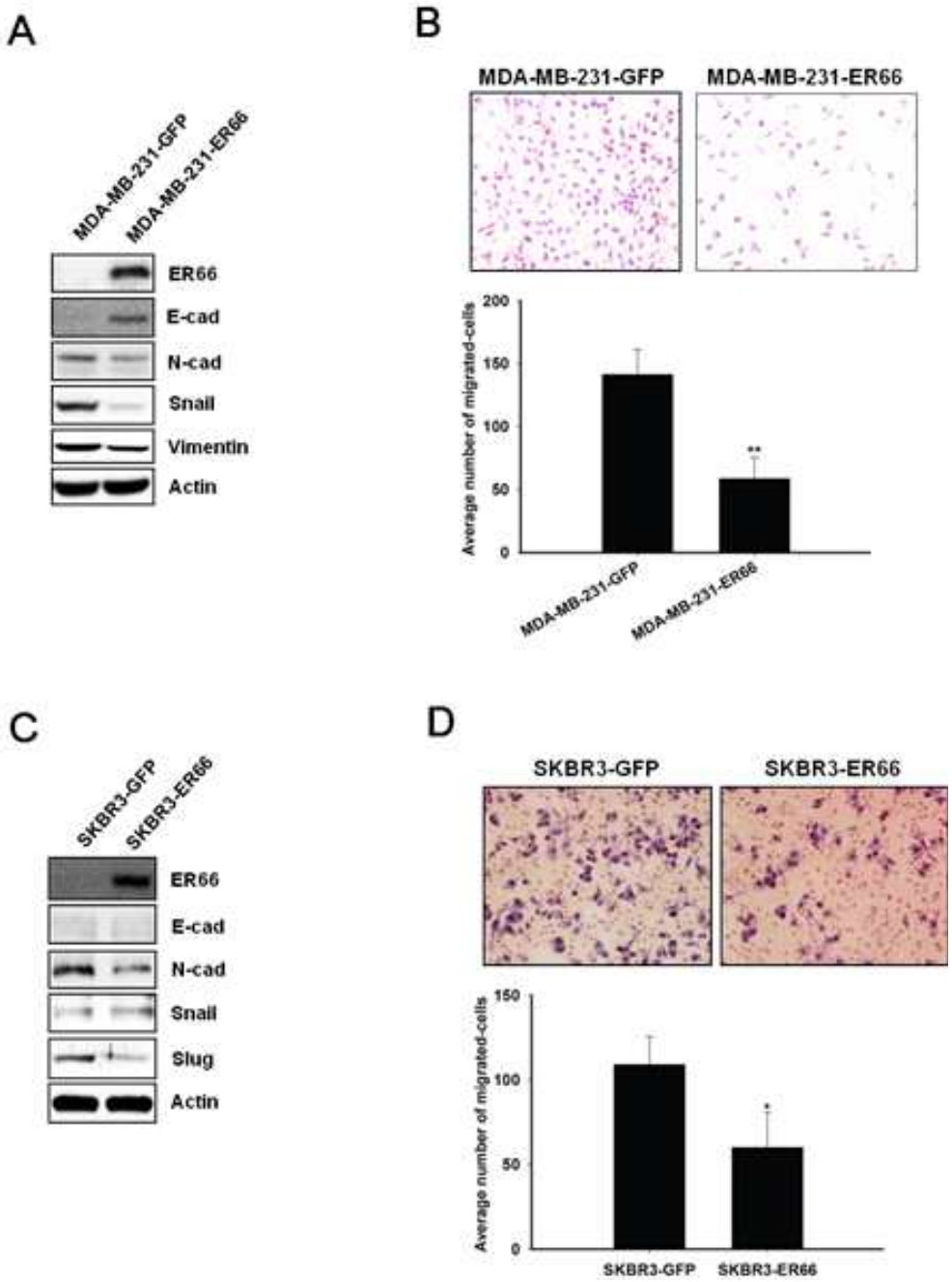

Fig. 14. Upregulation of ERα66 in ERα66-negative breast cancer cells suppresses EMT and migratory ability in vitro.

(A)(B) Overexpression of ERα66 in MDA-MB-231 cells.

(A) Immunoblot analyses of EMT markers in control MDA-MB-231-GFP cells and MDA-MB-231-ER66 cells.

(B) Trans-well migration assays demonstrating the reduction on migratory ability of ERα66-overexpressing MDA-MB-231 cells compared to control cells. Representative microscopy (× 20) images of MDA-MB-231-GFP cells and MDA-MB-231-ER66 cells (upper). The average migration cell number per field among different experimental groups (lower). Data represent the mean ± SD of three replicates ($^{**}p<0.01$, significant difference versus MDA-MB-231-GFP).

(C)(D) Overexpression of ERα66 in SKBR3 cells.

(C) Immunoblot analyses of EMT markers in control SKBR3-GFP cells and SKBR3-ER66 cells.

(D) Trans-well migration assays demonstrating the reduction on migratory ability of ERα66-overexpressing SKBR3 cells compared to control cells. Representative microscopy (× 20) images of SKBR3-GFP cells and SKBR3-ER66 cells (upper). The average migration cell number per field among different experimental groups (lower). Data represent the mean ± SD of three replicates ($^{*}p<0.05$, significant difference versus SKBR3-GFP).

1.15. Schematic diagram illustrating the role of ERα66 and ERα36 in TAMR-MCF-7 cells

Taken together, our finding illustrated the different roles of two ERα subtypes in breast cancer cells (Fig. 15). ERα36 is a key signaling factor for estrogen-independent growth and tumorigenesis of TAMR-MCF-7 cells. Overexpression of ERα36 induces downregulation of ERα66, subsequently acquires EMT and enhances cell migration. While ERα66 functionally plays as a crucial factor in maintenance of epithelial features in breast cells.

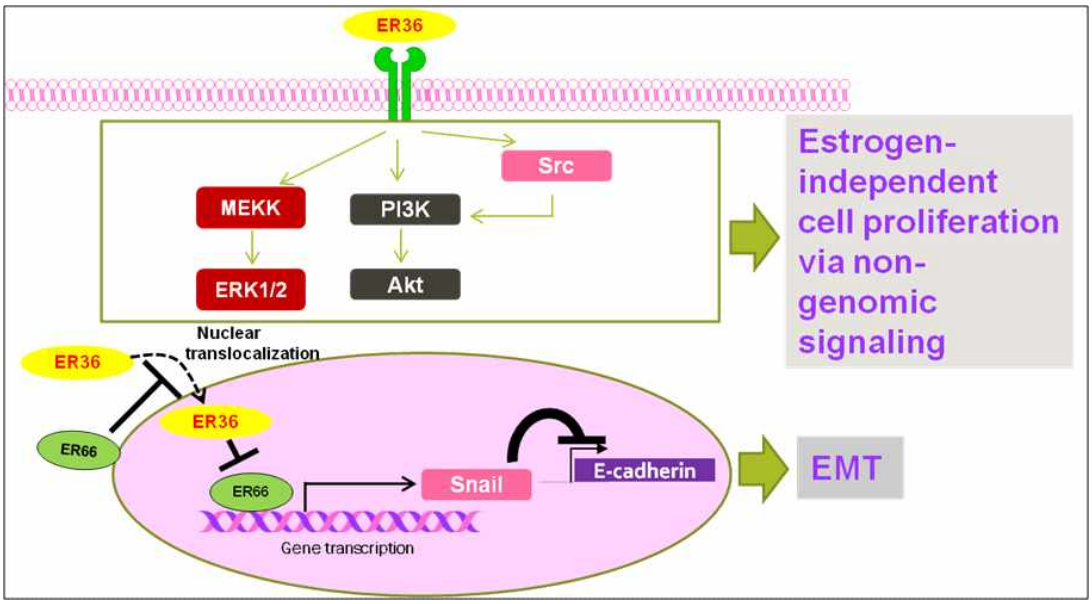

Fig. 15. Schematic diagram illustrating the role of ERα66 and ERα36 in TAMR-MCF-7 cells

Part 2: Role of Notch4/STAT3 signaling in epithelial-mesenchymal transition of Tamoxifen-resistant human breast cancer

2.1. Notch activation in TAM-resistant breast cancer is important for cell migration

Recently, Notch1 and Notch4 have emerged as prognostic markers for breast cancer [52]. Here, we observed that basal expression levels of Notch1 and especially Notch4 were significantly increased in TAMR-MCF-7 cells compared with control MCF-7 cells at both the mRNA and protein levels (Figs. 16A and 16B). Moreover, the ICDs of Notch1 and Notch4 were highly expressed in TAMR-MCF-7 cells (Fig. 16A). To confirm these findings in human, tumor tissues were obtained from two groups of patients. The group with no recurrence after TAM therapy (TAM-responsive group) included eight cases in whom no recurrence had occurred over at least 6 years of follow-up after mastectomy with adjuvant TAM therapy. The other group, the group with recurrence after TAM therapy (TAM-resistant group) included four cases who relapsed within 3 to 4 years after mastectomy with adjuvant TAM therapy. Immunohistochemistry showed that Notch1- or Notch4-positive staining was increased in cancer tissues from the TAM-resistant group compared with the TAM-responsive group (Fig. 16C).

To clarify the role of Notch signaling in TAMR-MCF-7 cells, DAPT, a potent Notch inhibitor, was used, and its effects on cell growth and migratory ability were examined. Because Harrison et al.

have reported that DAPT preferentially affect Notch1 activity in several types of cancer cells [53], we examined the effect of DAPT (0.3-10 μM on Notch4-ICD expression in TAMR-MCF-7 cells. DAPT (0.3-10 μM) treatment potently suppressed Notch4-ICD expression (Fig. 16D, upper panel). As shown in Fig. 16D lower panel, there was no significant change in the cell proliferation rate up to 72 h after DAPT treatment. However, trans-well migration assay showed that TAMR-MCF-7 cells possess greater in vitro migratory ability than the control MCF-7 cells, and this was significantly suppressed by DAPT exposure (Fig. 16E). Wound healing assay confirmed that DAPT treatment significantly inhibited wound density in TAMR-MCF-7 cells (Fig. 16F). These results imply that Notch activation in TAM-resistant breast cancer is critical for increased cell migration.

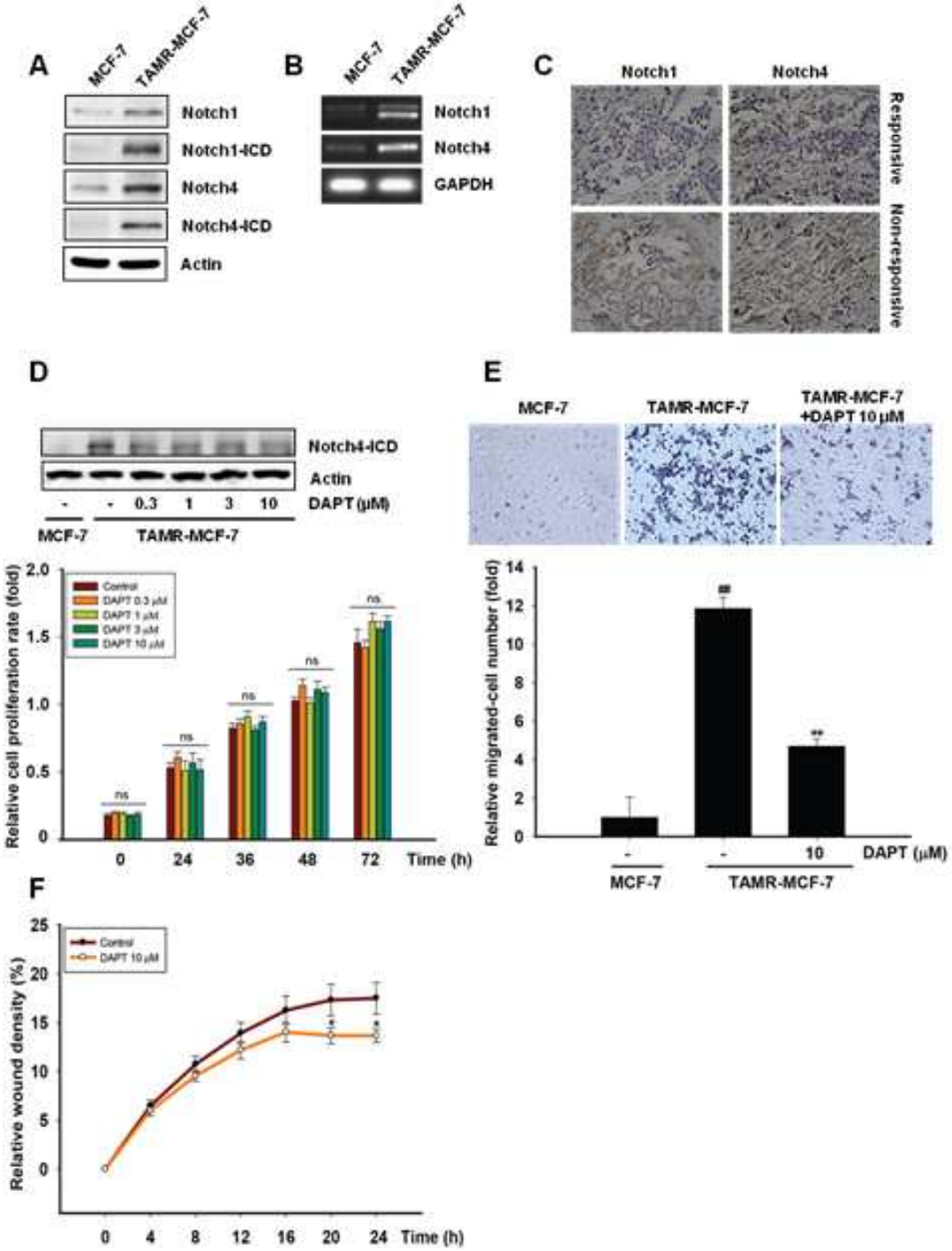

Fig. 16. Notch inhibitors suppress the migratory capacity of TAMR-MCF-7 cells.

(A) Protein expression of cleaved-Notch1 (Notch1-ICD), Notch1, cleaved-Notch4 (Notch4-ICD) or Notch4 in MCF-7 and TAMR-MCF-7 cells was determined by immunoblottings.
(B) The mRNA levels of Notch1 and Notch4 in MCF-7 and TAMR-MCF-7 cells were analyzed using RT-PCR analysis.
(C) Immunohistochemistry analyses of Notch1 and Notch4 were performed in Non-recurrence group after TAM therapy (TAM-responsive group, n=8) and Recurrence group after TAM therapy (TAM-resistant group, n=4), as shown in representative images (x 40 magnification).
(D) Upper; Effect of DAPT, a Notch inhibitor on Notch4-ICD expression in TAMR-MCF-7 cells. Lower; Effect of DAPT on cell proliferation of TAMR-MCF-7 cells. Cells were exposed to DAPT (0.3-10 μM) and cell proliferation was measured at different time points by MTT assay. Data represent mean ± SD with 6 different samples.
(E) Trans-well migration assays demonstrating the effect of DAPT on migratory ability of TAMR-MCF-7 cells. Representative microscopy images (× 20) of control MCF-7 cells, TAMR-MCF-7 cells and TAMR-MCF7 cells exposed to DAPT (upper). The number of migrated cells was counted and scored as relative unit (lower). Data represent the mean ± SD of three replicates ($^{\#\#}p<0.01$, significant difference versus MCF-7 cells; $^{**}p<0.01$, significant difference versus TAMR-MCF-7 cells; control level=1).
(F) Wound healing assay displaying the effect of DAPT on cell migration in TAMR-MCF-7 cells. Relative wound density was calculated by IncuCyte Chemotaxis Cell Migration Software. Data represent the mean ±SD (n=6) ($^{*}p<0.05$, significant difference versus vehicle-treated control cells).

2.2. Notch activation is involved in EMT progression in TAMR-MCF-7 cells

We have previously reported that TAMR-MCF-7 cells show typical morphological EMT features [6]. Western blot analyses revealed loss of the epithelial adhesion protein E-cadherin and upregulation of mesenchymal marker proteins such as N-cadherin and Snail in TAMR-MCF-7 cells (Fig. 17A). Correspondingly, immunocytochemical staining for E-cadherin showed high expression at the cell junctions in MCF-7 cells but no expression in the TAMR-MCF-7 cells (Fig. 17B).

To further validate the role of Notch related to EMT signaling in TAMR-MCF-7 cells, two different Notch inhibitors, DAPT and compound E, were used. The basal expression of N-cadherin and Snail in TAMR-MCF-7 cells was suppressed in a concentration-dependent manner by 24 h incubation with DAPT or compound E, while E-cadherin was not recovered by Notch inhibition (Fig. 17C). Interestingly, continuous exposure of TAMR-MCF-7 cells to 10 μM DAPT for 3 to 4 passages partially recovered E-cadherin expression in TAMR-MCF-7 cells (Fig. 17D). The reduction of mesenchymal markers such as N-cadherin and Snail were also observed in long-term culture of TAMR-MCF-7 cells with DAPT (Fig. 17D). Long-term treatment (3 to 4 passages) with DAPT led to remarkably decreased cell growth (Fig. 17E). When cultured on Matrigel (Corning Life Sciences, Corning, NY, USA) to assess the 3D growth potential, TAMR-MCF-7 cells displayed an aggressive phenotype, showing highly disorganized cell clusters lacking basal polarity, whereas the parent MCF-7 cells showed a more uniform and

polarized acinar structure. Meanwhile, TAMR-MCF-7 cells treated with DAPT formed more organized spheroid structures (Fig. 17F).

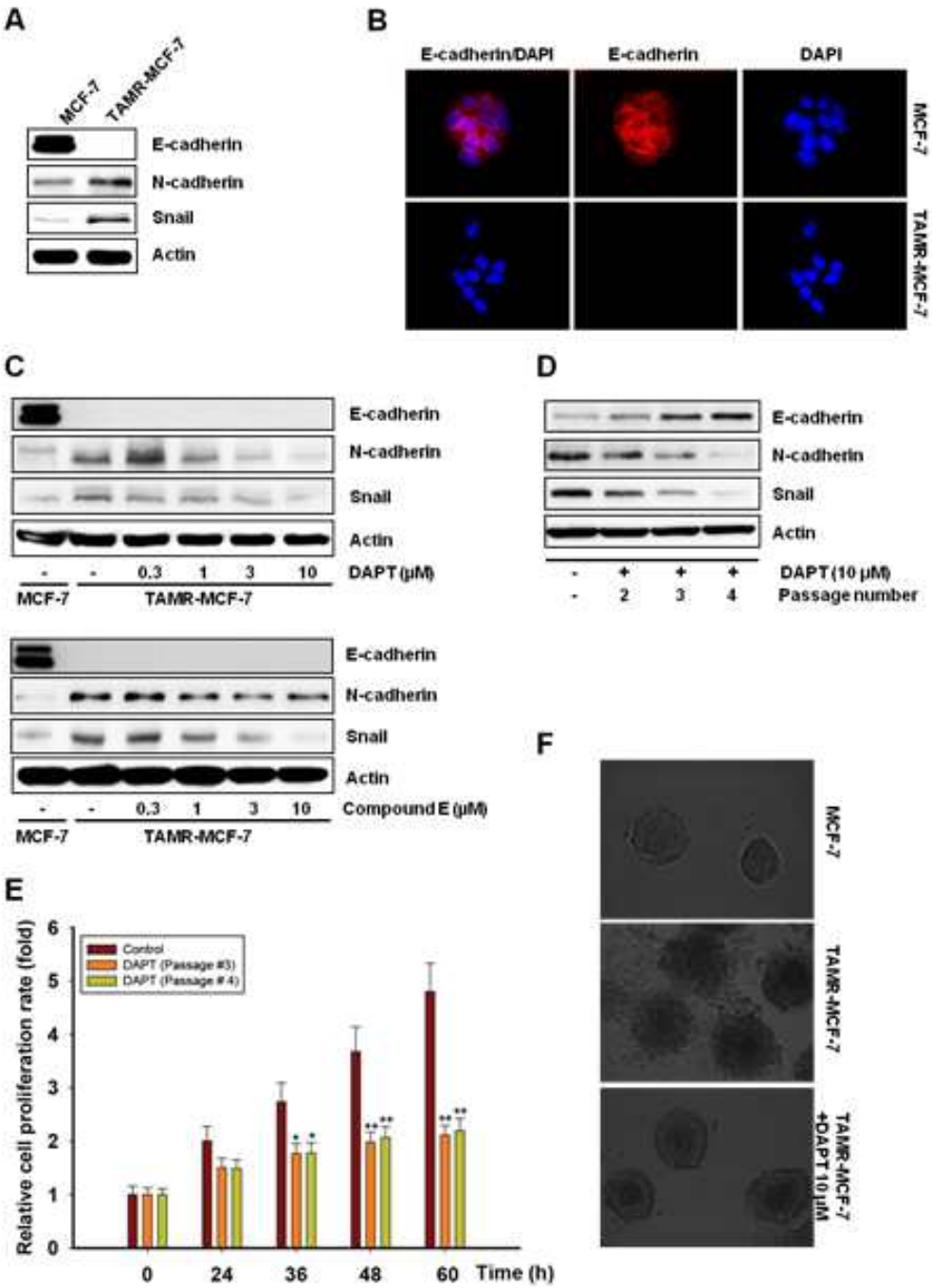

Fig. 17. Notch is involved in EMT progression in TAMR-MCF-7 cells.

(A) Immunoblot analyses of E-cadherin, N-cadherin and Snail in MCF-7 and TAMR-MCF-7 cells. (B) Representative E-cadherin staining in MCF-7 and TAMR-MCF-7 cells.

(C) Effects of Notch inhibitors, DAPT (upper) and compound E (lower) on the expression EMT markers.

(D) Reversal of EMT by long-term exposure (2-4 passages) of TAMR-MCF-7 cells to 10 μM DAPT.

(E) Cell proliferation rate of TAMR-MCF-7 cells continuously exposed to 10 μM DAPT (passage 3 or passage 4). Cell proliferation was measured at different time points by MTT assay and scored as relative unit. Data represent mean ± SD with 6 different samples ($^{*}p<0.05$, $^{**}p<0.01$, significant difference versus control cells; control level = 1).

(F) Spheroid formation of TAMR-MCF-7 cells in the presence or absence of DAPT (10 μM) when cultured in 3D-matrigel.

2.3. Notch4, but not Notch1, plays a critical role in EMT signaling in TAMR-MCF-7 cells

To investigate whether Notch1 and/or Notch4 is critical for EMT progression in TAMR-MCF-7 cells, the cells were transfected with control, Notch1 or Notch4 SMARTpool siRNA. Fig. 18A shows considerable suppression of Notch1 or Notch4 and their ICDs after transfection with each SMARTpool siRNA. Immunoblot analyses showed that the expression of N-cadherin and Snail, mesenchymal markers of EMT, was significantly reduced by Notch4 knockdown in TAMR-MCF-7 cells, whereas no changes were observed following Notch1 knockdown (Fig. 18B). These results demonstrate that Notch4 is important for EMT signaling in TAMR-MCF-7 cells. Moreover, Notch4 knockdown resulted in a marked reduction in migratory capacity in TAMR-MCF-7 cells, as evidenced by the trans-well migration assays (Fig. 18C).

To reduce the possibility of off-target effects of siRNA pooling, we also used two-independent siRNAs specifically targeting Notch4-ICD sequence. TAMR-MCF-7 cells transiently transfected with two Notch4-ICD-targeted siRNAs exhibited 80% or greater decrease in the protein levels of full-length Notch4 and Notch4-ICD when compared to control siRNA-transfected group, whereas the protein levels of Notch1 and its ICD form were marginally affected (Fig. 18D). Shown in Fig. 18E, both the siRNAs also inhibited the protein expression of N-cadherin and Snail in TAMR-MCF-7 cells.

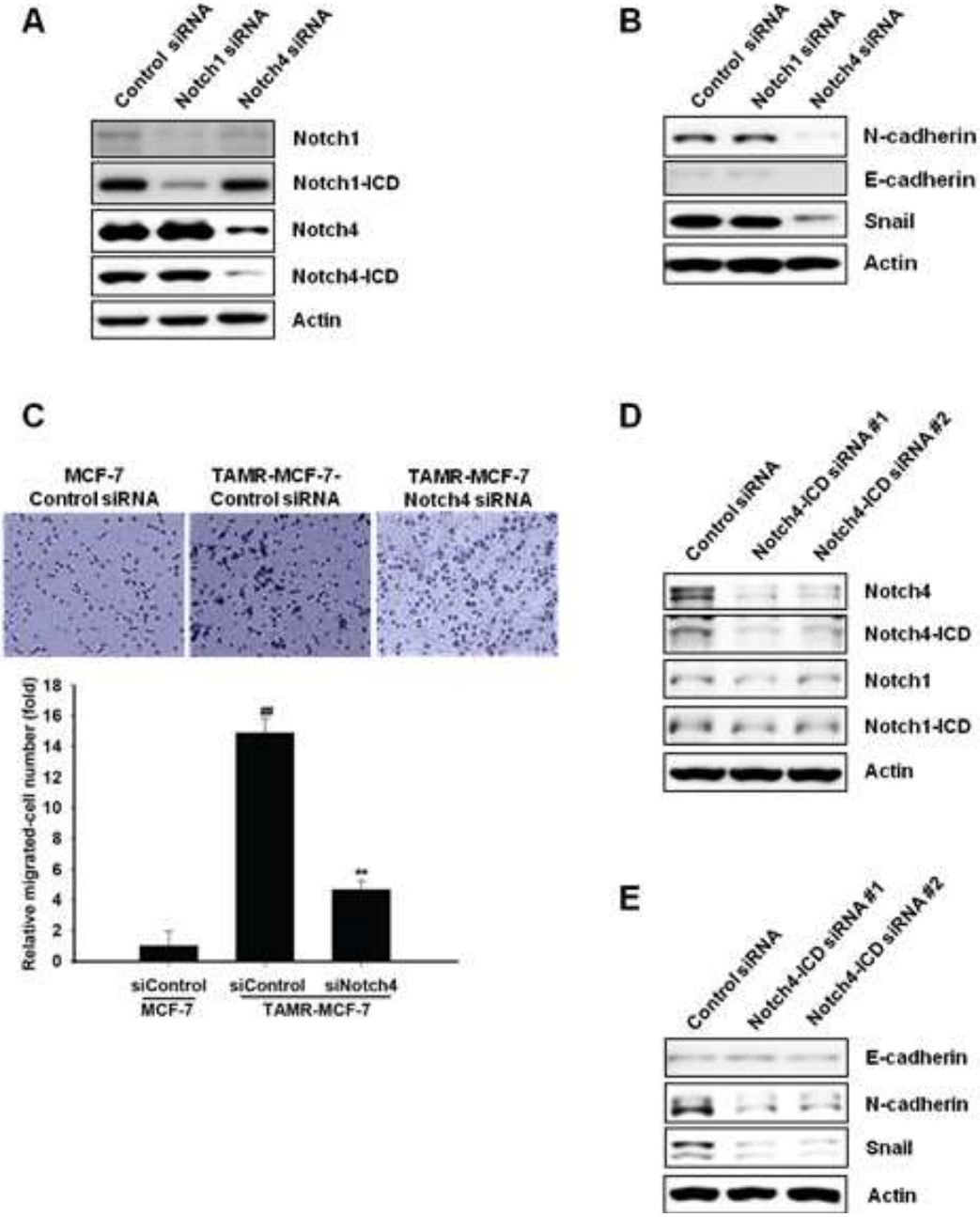

Fig. 18. Notch4, but not Notch1, plays a critical role in EMT signaling in TAMR-MCF-7 cells.

(A) MCF-7 and TAMR-MCF-7 cells were transfected with control or Notch1/4 siRNA for 48 h. Notch1/4 and their intracellular domain protein

levels were determined by immunoblottings.

(B) Immunoblot analyses of EMT markers after silencing of Notch1 or Notch4.

(C) The effect of Notch4 siRNA on the migratory ability of TAMR-MCF-7 cells was determined by trans-well migration assay. . Representative microscopy images (× 20) of MCF-7 cells and TAMR-MCF-7 cells transfected with either control siRNA or Notch4 siRNA (upper). The number of migrated cells was counted and scored as relative unit (lower). Data represent the mean ± SD of three replicates ($^{\#\#}p<0.01$, significant difference versus MCF-7 cells; $^{**}p<0.01$, significant difference versus TAMR-MCF-7 cells; control level = 1).

(D) Effects of Notch4-ICD sequence-specific siRNAs on the protein levels of Notch1/4 and their intracellular domains. TAMR-MCF-7 cells were transfected with control siRNA or Notch4-ICD siRNAs (#1 and #2) for 48 h. Notch1/4 and their intracellular domain protein levels were determined by immunoblottings.

(E) Immunoblot analyses of EMT markers after transfection of Notch4-ICD sequence-specific siRNAs.

2.4. Notch4/STAT3 crosstalk is important for EMT in TAMR-MCF-7 cells.

STAT3 is a transcription factor that regulates cell proliferation and survival and functions as a major driver of growth of stem cell-like breast cancer cells [54]. Activated or tyrosine-phosphorylated STAT3 plays a critical role in the regulation of tumorigenesis and metastatic spread of cancer cells [55]. Kamakura et al. [31] reported that STAT3 was activated in the presence of active Notch. Here, we also found that TAMR-MCF-7 cells had elevated levels of tyrosine 705-phosphorylated STAT3 (pY705) compared with the parent MCF-7 cells. Whereas, serine 727-phosphorylation of STAT3 was not altered between both cell types (Fig. 19A). To examine whether the constitutive phosphorylation of STAT3 in TAMR-MCF-7 cells is mediated by Notch signaling, Notch inhibitors were used. As shown in Fig. 20B, upregulation of activated STAT3 was attenuated by DAPT or compound E (Fig. 19B). To further verify the Notch subtype responsible for constitutive activation of STAT3, Notch1 and Notch4 knockdown was introduced. As shown in Fig. 19C, STAT3 phosphorylation was significantly decreased in Notch4-depleted TAMR-MCF-7 cells. However, Notch1 silencing did not have any effect on the phosphorylation of STAT3. Snyder et al. [56] demonstrated that Notch4 is one of the direct target genes of STAT3. Consistent with this finding, Stattic, a STAT inhibitor, considerably suppressed Notch4 and its ICD (Fig. 19D). On the contrary, STAT inhibition did not affect the expression of Notch1 or its ICD (Fig. 19D). Next, we explored the physical association between STAT3 and Notch4 or its ICD. Total cell lysates from

MCF-7 and TAMR-MCF-7 cells were immunoprecipitated using an anti-STAT3 antibody. Subsequent immunoblot analyses using Notch antibodies revealed that STAT3 physically interacts with the ICD of Notch4, and the interaction was enhanced in TAMR-MCF-7 cells compared with the control MCF-7 cells. However, there was no physical binding between full-length Notch4 and STAT3 (Fig. 19E). We also confirmed that Notch4 immunoprecipitates from both MCF-7 and TAMR-MCF-7 cells did not interact with STAT3 or P-STAT3 (data not shown). To identify the role of STAT3 in EMT progression in TAMR-MCF-7 cells, we examined the effect of STAT3 inhibitor on the expression of EMT markers. As expected, the protein expression of N-cadherin and Snail was suppressed by STAT3 inhibition (Fig. 19F).

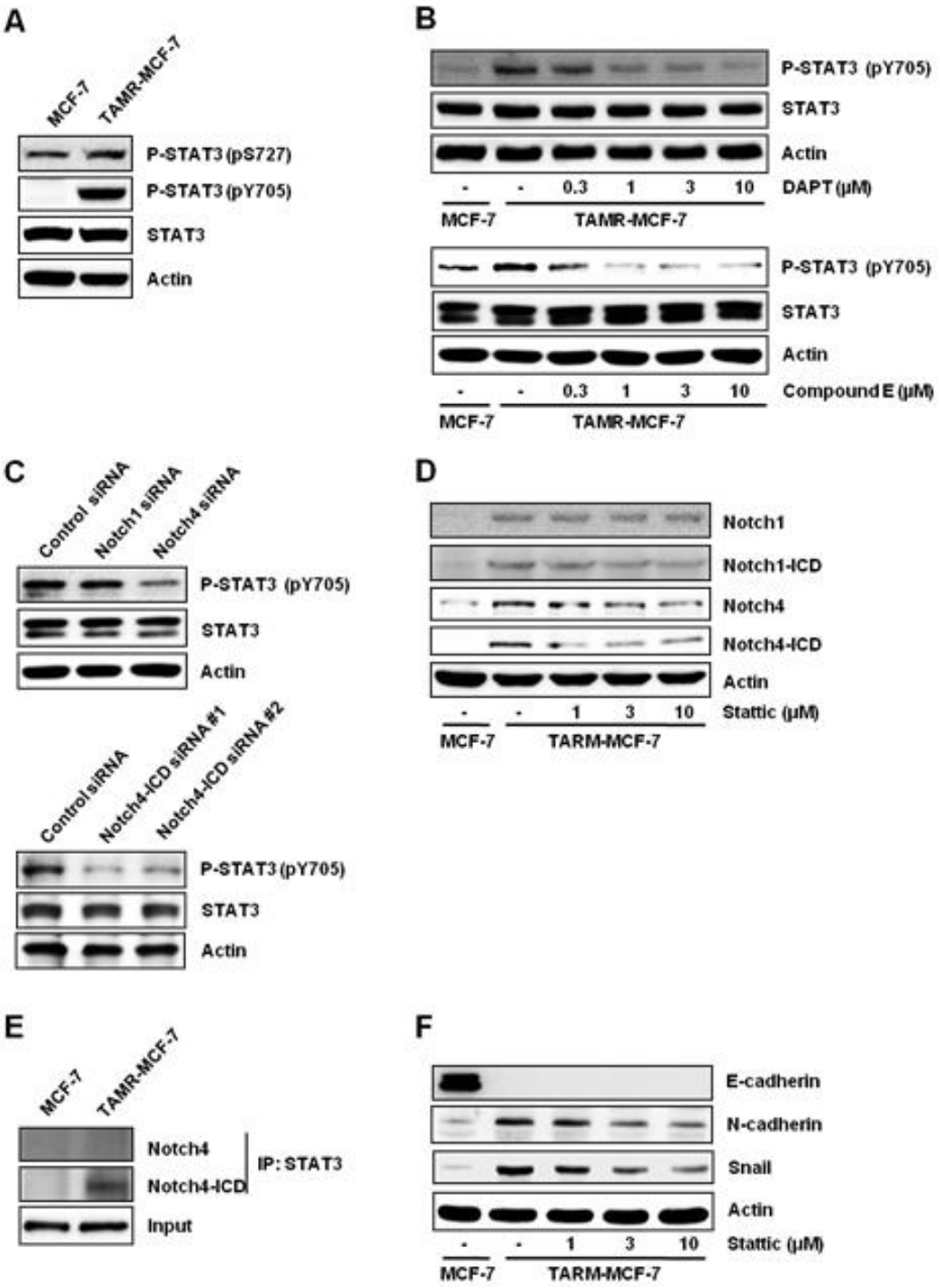

Fig. 19. Notch4/STAT3 crosstalk is important for EMT in TAMR-MCF-7 cells.

(A) Western blot analyses of Ser727- and Tyr705-phosphorylated STAT3.
(B) Effects of Notch inhibitors, DAPT (upper) and compound E (lower), on phosphorylated STAT3 (pY705) level.
(C) Effects of Notch1/4 siRNA (upper) and Notch4-ICD sequence-specific siRNAs (lower) on phosphorylated STAT3 (pY705) level.
(D) Effect of STAT inhibitor on the protein expression of Notch1/4 and their intracellular domains.
(E) STAT3 binding with intracellular domain of Notch4. Total cell lysates from MCF-7 and TAMR-MCF-7 cells were immunoprecipitated with STAT3 antiboty and immunoblotted with antibodies against Notch4 or Notch4-ICD.
(F) Immunoblot analyses of EMT markers in cells treated with STAT inhibitor, stattic.

2.5. Activation of Notch4/STAT3 upregulates MMP2 expression

Persistent activation of STAT3 governs the transcription of various target genes, including vascular endothelial growth factor and matrix MMPs, and subsequently controls many processes of cancer progression such as cell proliferation, angiogenesis, metastasis, immune evasion, and chemoresistance [57,58]. Direct binding of STAT3 to MMP2 regulates tumor invasion and metastasis [59]. Here, we observed that MMP2 was highly upregulated in TAMR-MCF-7 cells compared with the control MCF-7 cells (Fig. 20A). A recent study also demonstrated that Notch inhibition suppresses EMT progression with reduced TGFβ1- and angiotensin II-induced expression of MMP2 and Snail in human primary tubular epithelial cells [60]. In this study, DAPT and Stattic exposure resulted in reduced MMP2 mRNA levels in TAMR-MCF-7 cells (Figs. 20A and 20B). Reporter assays also confirmed that MMP2 transcription was suppressed by DAPT or Stattic treatment in a concentration-dependent manner (Figs. 20A and 20B). To further understand the molecular mechanism of activated Notch4/STAT3-driven MMP2 expression in TAMR-MCF-7 cells, we examined the transcriptional factors required for MMP2 induction in these cells. Transcription of MMP-encoding genes is regulated by their upstream sequences, including motifs corresponding to activator protein-1 (AP-1)- and nuclear factor-kappa B (NF-κB)-binding sites [61,62]. Although the MMP2 promoter does not contain NF-κB binding site, MMP2 is activated in tumor cells by an AP-1 or NF-κB-dependent pathway [62]. As expected, nuclear levels of c-Jun

and c-Fos (AP-1), which are upregulated in TAMR-MCF-7 cells, were inhibited by DAPT treatment (Fig. 20C). In addition, the enhanced AP-1 reporter activity in TAMR-MCF-7 cells was strongly suppressed by DAPT (Fig. 20C). Similar results were observed using a STAT3 inhibitor (Fig. 20D). Next, we examined nuclear p65 levels (NF-κB activity) in TAMR-MCF-7 cells incubated with a Notch or STAT inhibitor. There was a slight reduction in nuclear p65 levels following either DAPT or Stattic exposure (Figs. 20E and 20F). Inhibitory effects on NF-κB transcriptional activity was observed at a 10 μM, but not lower, concentration of the Notch or STAT inhibitor.

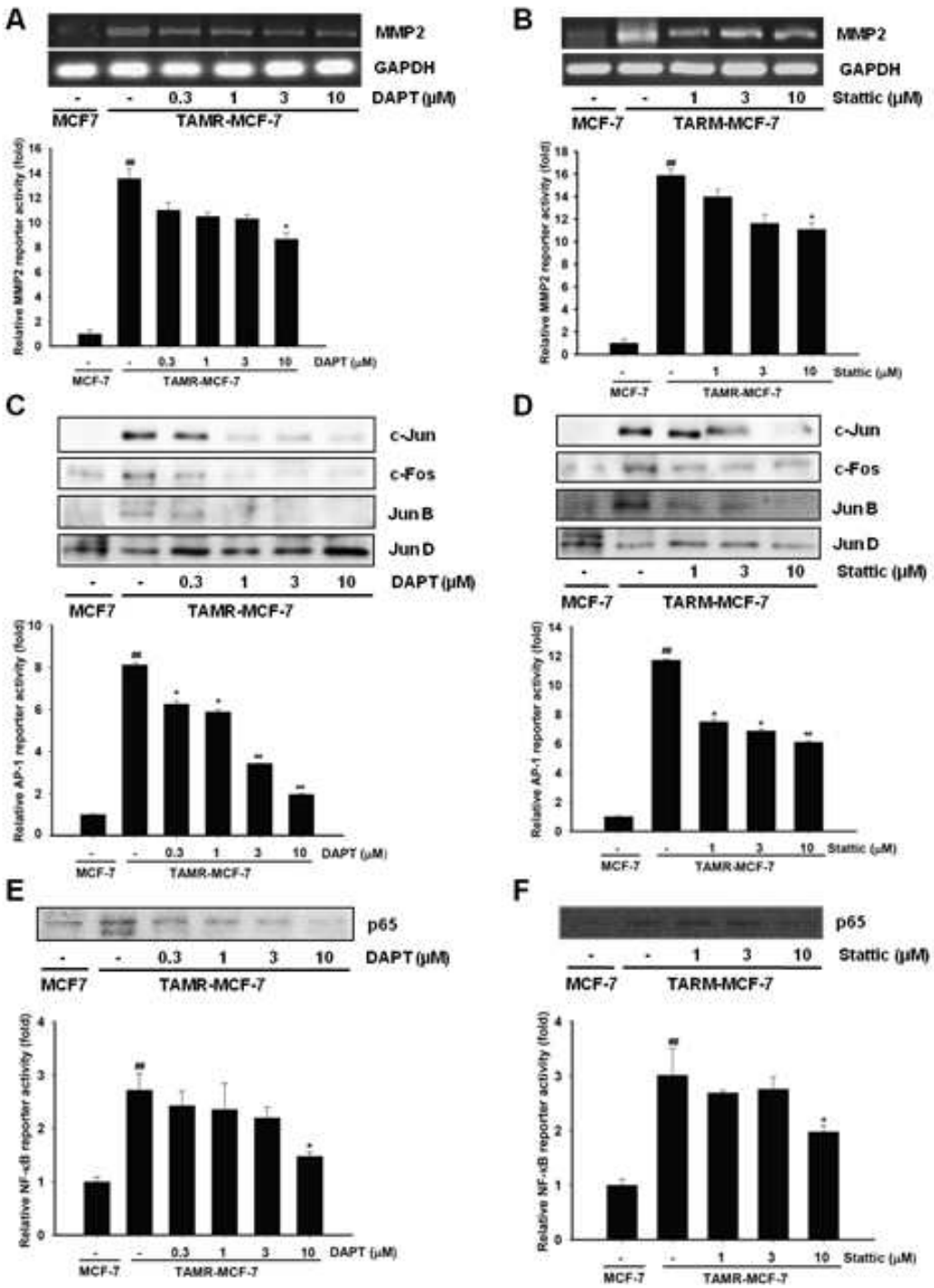

Fig. 20. Activation of Notch4/STAT3 signaling up-regulates MMP2.

(A) (B) Effects of Notch inhibition (A) or STAT inhibition (B) on mRNA expression and transcription of MMP2 gene. mRNA expression and transcriptional activity of MMP2 gene was determined by RT-PCR assay

(upper) and MMP2 promoter reporter activity (lower), respectively. MCF-7 and TAMR-MCF-7 cells were transiently transfected with MMP2-luc reporter (1 μg/ml) and phRL-SV (hRenilla) (1 ng/ml) plasmids. The transfected cells were incubated in serum-free medium. Reporter gene activity was calculated as a relative ratio of firefly luciferase to hRenilla luciferase activity. Data represent mean ± SD of 4 seperate samples ($^{\#\#}p<0.01$, significant as compared to MCF-7cells; $^{*}p<0.05$, significant as compared to TAMR-MCF-7 cells; control level = 1).

(C) Effect of Notch inhibitor on AP-1 activity in TAMR-MCF-7 cells. Upper panel, nuclear levels of c-Jun, c-Fos, Jun B and Jun D. Equal protein loading was verified by Ponceau S staining (data not shown). Lower panel, AP-1 reporter gene analysis. Data represent mean ± SD of 4 separate samples ($^{*}p<0.05$, $^{**}p<0.01$, significant as compared to MCF-7 cells; $^{\#\#}p<0.01$, significant as compared to TAMR-MCF-7 cells; control level = 1).

(D) Effect of STAT inhibitor on AP-1 activity in TAMR-MCF-7 cells. Upper panel, nuclear levels of c-Jun, c-Fos, Jun B and Jun D. Lower panel, AP-1 reporter gene analysis. Data represent mean ± SD of 4 separate samples ($^{\#\#}p<0.01$, significant as compared to MCF-7 cells; $^{*}p<0.05$, $^{**}p<0.01$, significant as compared to TAMR-MCF-7 cells; control level = 1).

(E) Effect of Notch inhibitor on NF-κB activity in TAMR-MCF-7 cells. Upper panel, nuclear levels of p65. Lower panel, NF-κB reporter gene analysis. Data represent mean ± SD of 4 separate samples ($^{\#\#}p<0.01$, significant as compared to MCF-7 cells; $^{*}p<0.05$, significant as compared to TAMR-MCF-7 cells; control level = 1).

(F) Effect of STAT inhibitor on NF-κB activity in TAMR-MCF-7 cells. Upper panel, nuclear levels of p65. Lower panel, NF-κB reporter gene analysis. Data represent mean ± SD of 4 separate samples ($^{\#\#}p<0.01$, significant as compared to MCF-7 cells; $^{*}p<0.05$, significant as compared to TAMR-MCF-7 cells; control level = 1).

2.6. A Notch inhibitor suppresses the micrometastatic tumor burden

We examined whether Notch inhibition suppresses metastasis of TAMR-MCF-7 cells *in vivo*. An intrasplenic injection model of liver metastases was performed. Mice were divided into three groups: mice bearing control MCF-7 cells and treated with the vehicle (group 1), mice bearing TAMR-MCF-7 cells and treated with the vehicle (group 2), and mice bearing TAMR-MCF-7 cells and treated with DAPT (10 mg/kg/day) via subcutaneous injection (group 3). There was no obvious difference in body weight among these three groups (Fig. 21A). Mice implanted with MCF-7 cells showed no tumor formation in the spleen and no liver metastases. On the contrary, mice implanted with TAMR-MCF-7 cells exhibited aggressive tumor formation in the spleen and increased susceptibility to macroscopic metastases on the liver surface (Fig. 21C). However, mice subcutaneously injected with DAPT (10 mg/kg/day) exhibited smaller tumors in the spleen and fewer macroscopic metastases in the liver (Figs. 21B and 21C). Only two of five mice in the DAPT-treated group displayed metastases, whereas macroscopic metastases appeared in four of five mice in the TAMR-MCF-7-implanted group with no drug exposure. Liver sections were stained with H&E to assess the metastatic tumor burden. As shown in Fig. 21D, liver tissues from mice implanted with TAMR-MCF-7 cells showed a metastatic tumor burden, but metastatic tumor formation was significantly decreased in the DAPT-injected group (Fig. 21D).

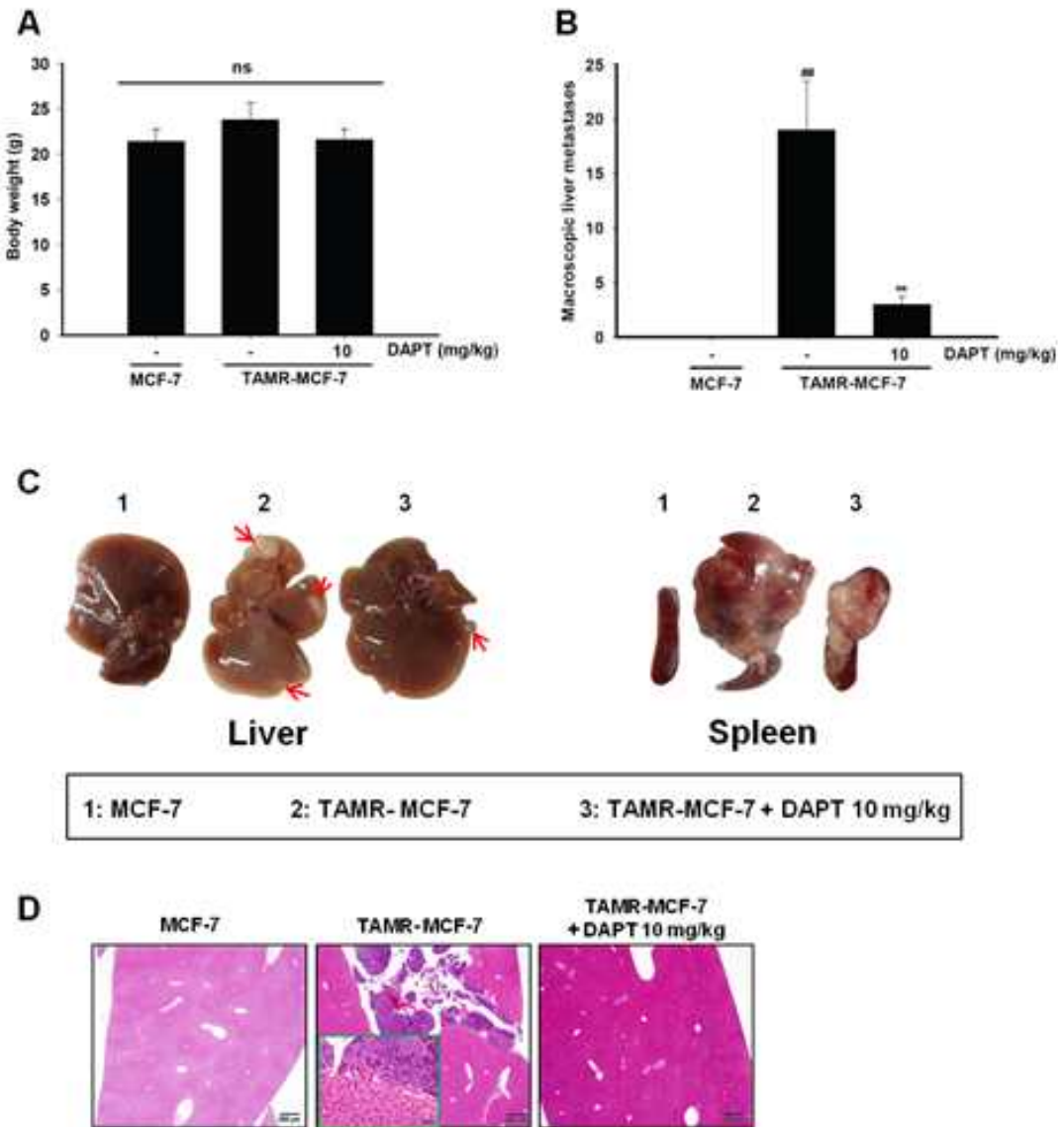

Fig. 21. Notch inhibition suppresses the micrometastatic tumor burden.

(A) Body weight was monitored on the day 28 after TAMR-MCF-7 cells inoculation.

(B) Numbers of macroscopic liver metastases were counted in mice bearing control MCF-7 and TAMR-MCF-7 cells. The mice inoculated with TAMR-MCF-7 cells were divided into two groups and subcutaneously injected with vehicle (30% polyethyleneglycol 400 in saline) and DAPT (10 mg/kg). Data represents mean ± SD (n=5)($^{\#\#}p<0.01$, significant as compared

to mice implanted with MCF-7 cells; $^{**}p<0.01$, significant as compared to mice implanted with TAMR-MCF-7 cells; control level = 1).

(C) Representative macroscopic liver metastases. Red arrow indicates macroscopic metastases identified on the surface of livers.

(D) Representative images of H&E-stained liver sections from each group.

2.7. Expression of Notch1 and Notch4 in breast cancer cells

We raised the question whether Notch associated with ERα expression in mediating EMT signaling. We then examined the expression of Notch4 in ERα66-overexpressing TAMR-MCF-7 cells. No remarkable difference of Notch1 and Notch4 expression was observed between TAMR-ER66 cells and mock-transfected TAMR-MCF-7 cells (Fig. 22A). Interestingly, both Notch1, Notch4 and their ICDs were upregulated in ERα36-overexpressing MCF-7 cells in 10% FBS-stimualated condition whereas no change were found with Notch1, Notch1-ICD and Notch4 in estrogen-deprived condition (Fig 22B). However, Notch4-ICD was slightly higher in MCF7-ER36 cells compared to control MCF7-pcDNA3.1 cells. Silencing of ERα36 in TAMR-MCF-7 cells resulted in significant suppression of Notch1, Notch4 and their ICDs (Fig. 22C). These data imply that Notch signaling may be related to ERα36 and the expression of Notch in ERα36-overexpressing MCF-7 cells is estrogen-dependent manner. Further studies should be performed for better understanding about the correlation between Notch and ERα.

.

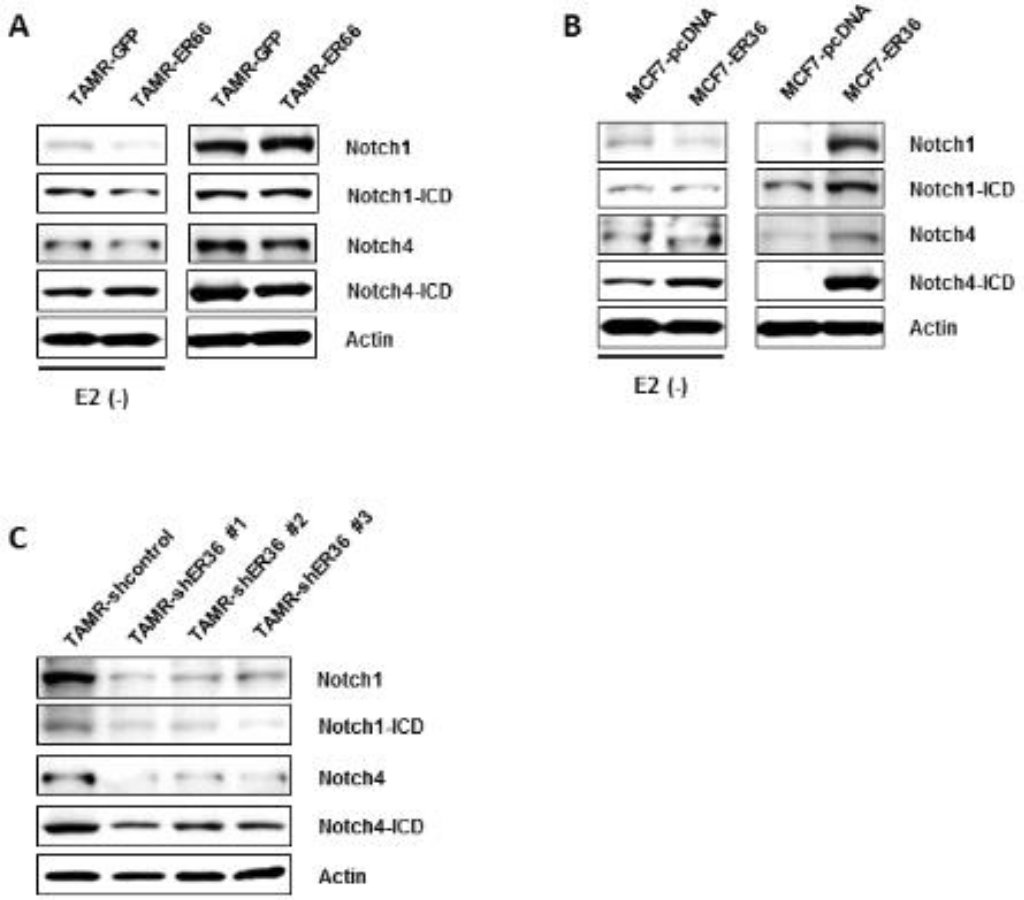

Fig. 22. Expression of Notch1and Notch4 in breast cancer cells.

(A) Western blot analyses of Notch1-ICD, Notch1, Notch4-ICD or Notch4 in TAMR-GFP cells and TAMR-ER66 cells in estrogen-deprived condition or 10% FBS-stimulated condition.

(B) Immunoblot analyses of Notch1-ICD, Notch1, Notch4-ICD or Notch4 in MCF7-pcDNA3.1 cells and MCF7-ER36 cells in estrogen-deprived condition or 10% FBS-stimulated condition.

(C) Immunoblot analyses of Notch1-ICD, Notch1, Notch4-ICD or Notch4 in control TAMR-shc cells and TAMR-shER36 cells.

2.8. Schematic illustration of the molecular mechanism of Notch4/STAT3 signaling in mediating EMT

Collectivelly, our findings reported for the first time the crosstalk between Notch4 and STAT3 in the regulation of EMT signaling in TAM-resistant breast cancer (Fig. 23). Notch4/STAT3 activation in TAMR-MCF-7 cells is critical to MMP2-dependent cell migration and Notch4 could be a promising therapeutic target for preventing metastasis in TAM-resistant breast cancer.

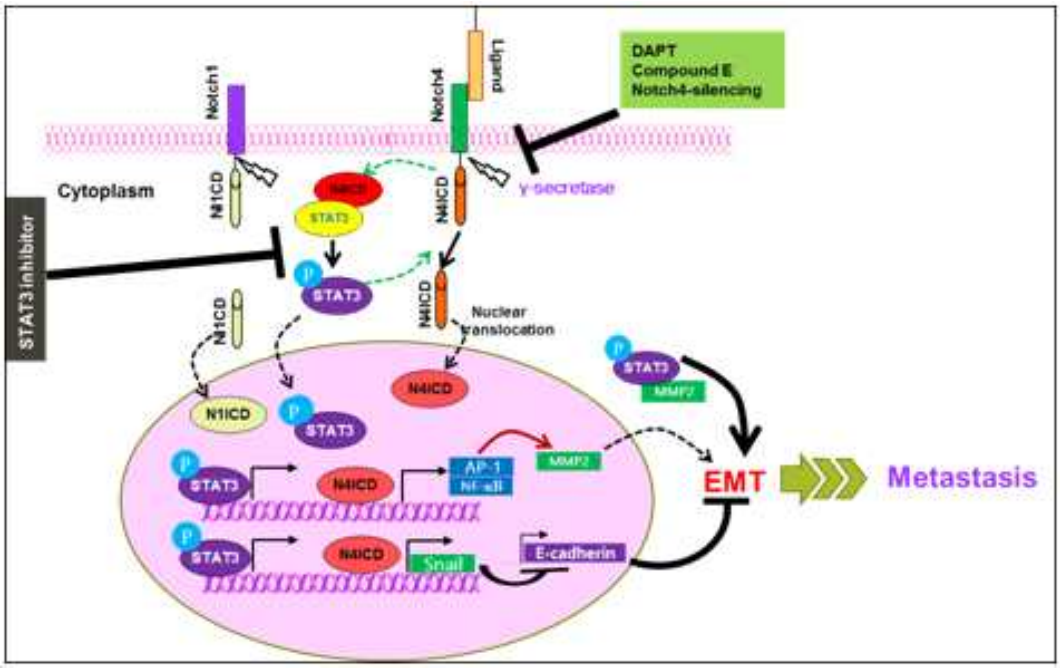

Fig. 23. Proposed mechanism for Notch4/STAT3 signaling in the regulation of EMT process in tamoxifen-resistant breast cancer cells

IV. DISCUSSION

It has been reported that critical milestones in the phenotypic progression of ERα-positve breast tumors include a loss of hormone-dependence and an increased metastatic potential [5, 63]. EMT is considered as a phenotypic conversion linked with metastasis [64,65]. In the EMT processes, epithelial cells gain mesenchymal properties, loose intercellular adhesion and increased motility; subsequently they may have capacity to break through the basal membrane and migrate over long distances owing to profound changes in their cytoskeleton architecture [64].

A hallmark of EMT is losing expression of E-cadherin, a key cell-cell coherence molecule, which is recognized as a caretaker of the epithelial phenotype [8-10]. Several studies have revealed the association of some characteristics of EMT with ERα status in tamoxifen-resistent breast cancer cells [18,20,41,42,49]. Our study also demonstrated the upregulation of ERα36 and loss of ERα66 expression in TAMR-MCF-7 cells. It has been shown that the cytoplasmic expression of ERα66 was frequently observed in ERα36-positive breast cancer tissues, while in ERα66-positive breast cancer tissues, ERα66 is primarily expressed in the nucleus [20]. Our data displayed that ectopic expression of localized ERα66 could inhibit the nuclear distribution of ERα36 in TAMR-MCF-7 cells. These findings suggests a possible regulatory interaction between the two variants of ERα.

It has been also revealed that ERα36 upregulation played an important role in this growth status switch [16]. Our finding clearly

indicated that ERα36 overexpression was involved in EMT-dependent cell migration by inducing downregulation of ERα66. Because ER36 is primary distributed in plasma membrane and cytoplasm, it may be related with the activation of non-genomic signaling of ER. However, when we compared cell proliferation of ERα36-overexpressing MCF-7 cells with mock-transfected MCF-7 cells, estrogen-dependent cell proliferation was not significantly changed. On the contrary, estrogen-independent cell proliferation in ERα36-overexpressing MCF-7 cells was remarkably higher than control cells. Moreover, mouse xenograft modelling of both MCF7-ER36 cells and TAMR-MCF-7 cells caused rapid tumor growth in mice that had to be killed before the control cells reached comparable sizes of tumors. However, metastasis did not appeared on the surface of the liver despite MCF7-ER36 cells caused aggressive tumor formation in spleen in intrasplenic injection model of liver metastases. Hence, ERα 36 is a key signaling factor for estrogen-independent growth and tumorigenesis of TAMR-MCF-7 cells.

Loss of ERα66 in breast cancer cells results in EMT progression characterized by remarked changes in the expression profile of EMT markers and the reorganization of F-actin [49]. Upregulation of ERα 66 eventually reverses the EMT to MET in ERα66-negative breast cancer cells and suppresses cell migration. Our data are consistent with previous report, ERα66 suppresses the expression of the nuclear transcription factor Snail, a negative transcription factor of E-cadherin gene expression [66]. These denoted that ERα66 functionally plays as a crucial factor in maintenance of epithelial features in breast cancer cells. Nevertheless, ERα66-overexpressing TAMR-MCF-7 cells were still exhibited the comparable capacity of tumorigenesis and

metastasis with mock-transfected TAMR-MCF-7 cells. It has recently been reports have been shown that EMT is not required for metastasis but induces chemoresistance in pancreatic cancer [67]. Fisher et al. have also demonstrated that highly proliferative non-EMT cells are sensitive to chemotherapy, and observe the emergence of recurrent EMT-derived metastases after treatment in spontaneous breast-to-lung metastasis models [68]. The study also revealed that blockade of EMT signaling may not affect metastasis formation [68]. These new findings suggested the potential of an EMT-targeting strategy, in combination with conventional chemotherapies, to combat chemoresistance [67,68].

Binding of Notch ligand (Jagged or Delta) to the extracellular domain of Notch receptor induce proteolytic cleavage (γ-secretase) and release its intracellular domain (NICD), which translocates to the nucleus to modify transcription of its target genes, then regulates migration and invasion of breast cancer cells [22,27,28]. Rizzo et al. revealed that γ-secretase inhibitors block the proliferative effect of tamoxifen through the Notch pathway, and at the same time allow tamoxifen to exert its antagonistic effect [23]. However, crosstalk between Notch and ER signaling are still elusive.

The Notch signaling pathway is abberantly activated in breast cancer stem cells [53], and this process is associated with TAM resistance [69]. In addition, Jag1/Notch4 signaling in human breast tumors is an important driver of CSCs [69]. Our study demonstrated the increased Notch1 and Notch4 expression in TAMR-MCF-7 cells compared with parental MCF-7 cells. In human cases, tumor tissues obtained from the TAM-resistant group showed elevated Notch1 and Notch4 levels compared with the TAM-responsive group. It is also

consistent with recent reports showing that Notch4 expression is increased in endocrine-resistant breast cancer cells [54,69]. We also found that overexpression of ERα36 in MCF-7 greatly upregulated Notch4-ICD expression.

There is crosstalk between Notch and several growth factors relevant to EMT, and this crosstalk modulates the activities of many signaling pathways that contribute to the establishment of migratory and invasive mesenchymal phenotypes [22,30]. Downregulation of E-cadherin expression reduces cell - cell adhesion, leading to modifications from an epithelial to mesenchymal phenotype [7]. Recent studies showed that overexpression of the Notch-ICD alone increased Snail expression and resulted in the loss of E-cadherin [60]. Meanwhile, suppression of Notch signaling abrogated the reduced E-cadherin and Snail expression [60]. We have previously shown that PTEN/PI3-kinase/Akt/GSK-3β-dependent Snail activation and/or NF-κB activation are involved in EMT processes of TAMR-MCF-7 cells [6]. In agreement with this finding, EMT markers and migratory capacity were significantly attenuated in TAMR-MCF-7 cells by either Notch inhibitors or Notch4 knockdown. Especially, continuous exposure to DAPT, a Notch inhibitor, over several passages eventually led to partial reversal of EMT by restoring E-cadherin expression in TAMR-MCF-7 cells. Our data indicate that Notch4, but not Notch1, plays an important role in mediating EMT processes in TAMR-MCF-7 cells. This finding is consistent with a recent report that Notch4-ICD overexpression in HMEC-1 endothelial cell line causes loss of endothelial phenotype and potential transformation to mesenchymal cells [70]. In addition, Lombardo et al. also demonstrated that Notch4 upregulation promotes the EMT signaling

in TAM-resistant breast cancer cells [30].

Constitutive activation of STAT3 occurs during the progression of numerous human cancers, including breast cancer [32]. Recent studies have shown that Notch1 signaling induces STAT3 phosphorylation and participates in EMT [71,72]. A wide range of cytokines, growth factors, and oncogenic stimuli can activate STAT3 by regulating diverse sets of posttranslational modification including tyrosine and serine phosphorylation [73]. In response to ligand stimulation, phosphorylation of specific residue (Tyr705 or Ser727) determines the activity of STAT3 [74-77]. Phosphorylation of Tyr705 stimulates STAT3 dimerization with other STATs, which leads to nuclear translocation and DNA binding. Phosphorylation of Ser727 locating at the C-terminal transactivation domain of STAT3 is mediated by various serine kinases such as mitogen-activated protein kinases, cyclin-dependent kinases, and protein kinase C [77,78]. It has been reported that Tyr705 phosphorylation is critical for STAT3 function, whereas Ser727 phosphorylation has both stimulating and inhibitory effects on gene transcription [74-77]. In ovarian cancer, Snail-dependent EMT is controlled by Tyr705 phosphorylation of STAT3 [79]. Here, we showed that TAMR-MCF-7 cells exhibited enhanced phosphorylation of STAT3 at the tyrosine 705 residue. Notch inhibitors suppressed activation of STAT3. Consistent with that, silencing of Notch4 or Notch4-ICD downregulated phosphorylation of STAT3 in TAMR-MCF-7 cells. On the other hand, a STAT3 inhibitor also displayed an inhibitory effect on the formation of cleaved Notch4 and led to the suppression of EMT markers. These results support our hypothesis that Notch4 mediates the EMT modifications observed in TAMR-MCF-7 cells via STAT3

signaling. To our knowledge, this is the first report of crosstalk between Notch4 and STAT3 in the regulation of EMT signaling.

STAT3 activation is correlated with enhanced activity of MMP2, which is itself a STAT3 target gene, and blockade of STAT3 activity by dominant-negative mutant of STAT3 or treatment with a JAK inhibitor reduced MMP activity [59]. Transcription of Notch4 gene in endothelial cells is triggered by the AP-1 pathway [80]. Notch signaling, as indicated by Notch protein cleavage, is mediated by NF-κB activation, and the canonical NF-κB-binding motif 5'-GGRRNNYYCC-3' exists in the promoters of DLL4, Notch1 and Notch4 genes [81]. In this study, either Notch or STAT inhibition reduced MMP2 mRNA levels and reporter activity in TAMR-MCF-7 cells. Simultaneously, the nuclear expression and transcriptional activities of AP-1 and NF-κB were suppressed by both DAPT and Stattic. As MMP2 activation is important in cell invasion through degradation of the extracellular matrix and basement membrane, our results suggest that Notch4/STAT3 activation in TAMR-MCF-7 cells is also critical to MMP2-dependent cell migration.

Furthermore, the intrasplenic injection model of liver metastases showed that TAMR-MCF-7 cells had a high capacity to form tumors within the spleen and macroscopic metastases on the surface of the liver. Interestingly, mice receiving daily DAPT treatment showed a decreased hepatic tumor burden. Our study thus indicates the fundamental function of Notch4/STAT3 on EMT signaling and demonstrates that Notch4 could be a promising therapeutic target for preventing metastasis in TAM-resistant breast cancer.

It has been reported that ER-targeted endocrine therapies may raise the number of ERα66-negative cells during acquired resistance

[82,83]. Combination therapies targeting both Notch and ERα66 to preserve cells in an ERα-positive luminal state could be a potential therapeutic approach for the treament of ERα66-positive breast cancer and such a combination possibly defeat the emergence of tamoxifen-resistance [83,84]. Experimental evidence also indicated that targeting Notch could overcome drug resistance of cancer cells, which may lead to the destruction of CSCs or EMT phenotype which are considered as the “root cause” of tumor recurrence [23].

Howerver, long-term treatment with Notch inhibitors may cause some risks. One possibility is the damage of normal stem cells, which may rely on Notch signaling. The consequence of this impact is hard to accurately evaluate, but could include anything from hematopoietic collapse to subtle cognitive decline [85]. The other risk may be even more concerning, the increased incidence of certain cancers. While Notch frequently acts as an oncogenic molecule, it may also be considered as a tumor suppressor in some cell types, such as skin cells, neuroendocrine lung cells and B-cells [86-88]. Hence, continuously expose to Notch inhibitor may increase the risk of cancers in these cellular compartments. Despite the potential risks, Notch inhibitor seems to be well-tolerated and Notch has become one of the most promising target in cancer therapies [85].

Besides that, there has no report about the correlation of ERα status and Notch4 expression so far. We then examined the expression of Notch4 in ERα66-overexpressing TAMR-MCF-7 cells. No remarkable association was observed in TAMR-ER66 cells and control TAMR-GFP cells. Interestingly, the expression of both Notch1 and Notch4 in ERα36-overexpressing MCF-7 cells are hormone-dependent manner. Further studies should be performed for

better understanding about the correlation between Notch4 and ERα36.

In conclusion, our data demonstrated that ERα66 is responsible for preserving cells from epithelial to mesenchymal transition process in ERα-positive breast cancer cells. Notch4/STAT3 signaling pathway plays a key role in EMT progression during acquired tamoxifen resistance acquisition in human breast cancer.

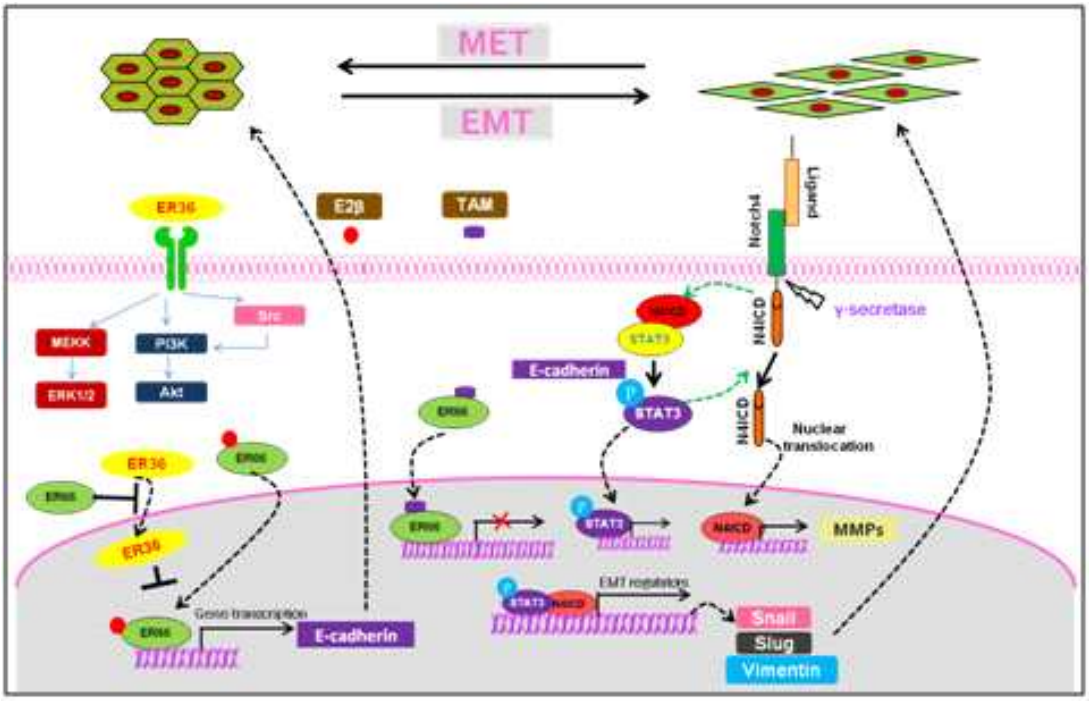

Fig. 24. A schematic diagram illustrating the role of ERα66 and Notch4/STAT3 signaling in mediating EMT phenotype of tamoxifen-resistant breast cancer cells

V. REFERENCES

1. Ferlay J, Soerjomataram I, Ervik M, et al. GLOBOCAN 2012 cancer incidence and mortality worldwide: IARC cancerbase No. 11. Lyon, France: International Agency for Research on Cancer, 2013.

2. Harvey JM, Clark GM, Osborne CK, Allred DC. Estrogen receptor status by immunohistochemistry is superior to the ligand-binding assay for predicting response to adjuvant endocrine therapy in breast cancer. J Clin Oncol. 1999; 17: 1474-1481.

3. Jaiyesimi IA, Buzdar AU, Decker DA, Hortobagyi GN. Use of tamoxifen for breast cancer: twenty-eight years later. J Clin Oncol. 1995; 13: 513-529.

4. Díaz-Cruz ES, Shapiro CL, Brueggemeier RW. Cyclooxygenase inhibitors suppress aromatase expression and activity in breast cancer cells. J Clin Endocrinol Metab. 2005; 90: 2563-2570.

5. Clarke R, Thompson EW, Leonessa F, Lippman JMS McGarvey M, Frandsen TL et al. Hormone resistance, invasiveness, and metastatic potential in breast cancer. Breast Cancer Res Treat. 1993; 24: 227-239.

6. Kim MR, Choi HK, Cho KB, Kim HS, Kang KW. Involvement of Pin1 induction in epithelial-mesenchymal transition of tamoxifen-resistant breast cancer cells. Cancer Sci. 2009; 100: 1834-1841.

7. Christiansen JJ, Rajasekaran AK. Reassessing epithelial to mesenchymal transition as a prerequisite for carcinoma invasion and metastasis. Cancer Res. 2006; 66: 8319-8326.

8. Moreno-Bueno G, Portillo F, Cano A. Transcriptional regulation of

cell polarity in EMT and cancer. Oncogene. 2008; 27: 6958-6969.
9. Hazan RB and Norton L: The epidermal growth factor receptor modulates the interaction of E-cadherin with the actin cytoskeleton. J Biol Chem. 1998; 273: 9078-9084. 1998.
10. Cheng CW, Wu PE, Yu JC, et al: Mechanisms of inactivation of E-cadherin in breast carcinoma: modification of the two-hit hypothesis of tumor suppressor gene. Oncogene. 2001; 20:3814-3823.
11. Yoshida R, Kimura N, Harada Y and Ohuchi N: The loss of E-cadherin, α- and β-catenin expression is associated with metastasis and poor prognosis in invasive breast cancer. Int J Oncol. 2001; 18: 513-520.
12. Parker C, Rampaul RS, Pinder SE, et al: E-cadherin as a prognostic indicator in primary breast cancer. Br J Cancer. 2001; 85: 1958-1963.
13. Kowalski PJ, Rubin MA and Kleer CG: E-cadherin expression in primary carcinomas of the breast and its distant metastases. Breast Cancer Res. 2003; 5: R217-R222.
14. Wang ZY, Zhang XT, Shen P, Loggie BW, Chang Y, Deuel TF. Identification, cloning, and expression of human estrogen receptor-alpha 36, a novel variant of human estrogen receptor-alpha 66. Biochem Biophys Res Commun. 2005; 336:1023-1027.
15. Lee LMJ, Cao J, Deng H, Chen P, Gatalica Z, Wang ZY. ER-α36, a novel variant of ER-α, is expressed in ER-positive and -negative human breast carcinomas. Anticancer Res. 2008; 28: 479-483.
16. Wang ZY, Zhang XT, Shen P, Loggie BW, Chang Y, Deuel TF. A variant of estrogen receptor-alpha, hER-alpha 36: transduction of estrogen- and antiestrogen-dependent membrane-initiated mitogenic signaling. Proc Natl Acad Sci USA. 2006; 103: 9063-9068.

17. Zhang X, Ding L, Kang L, Wang ZY. Estrogen receptor-alpha 36 mediates mitogenic antiestrogen signaling in ER-negative breast cancer cells. PLoS One. 2012; 7: e30174.
18. Li G, Zhang J, Jin K, He K, Zheng Y, Xu X, et al. Estrogen receptor-α36 is involved in development of acquired tamoxifen resistance via regulating the growth status switch in breast cancer cells. Mol Oncol. 2013; 7: 611-624.
19. Kang L, Guo Y, Zhang X, Meng J, Wang ZY. A positive cross-regulation of HER2 and ER-α36 controls ALDH1 positive breast cancer cells. J Steroid Biochem. 2011; 127: 262-8.
20. Shi L, Dong B, Li Z, Lu Y, Ouyang T, Li J et al. Expression of ER-α36, a novel variant of estrogen receptor α, and resistance to tamoxifen treatment in breast cancer. Journal of Clinical Oncology. 2009; 27: 3423-3429.
21. Stylianou S1, Clarke RB, Brennan K. Aberrant activation of notch signaling in human breast cancer. Cancer Res. 2006; 66:1517-1525.
22. Kevin GL, Aly K. Recent insights into the role of Notch signaling in tumorigenesis. Blood. 2006; 107: 2223-2233.
23. Rizzo P, Miao H, D'Souza G, Osipo C, Song LL, Yun J et al. Crosstalk between Notch and the estrogen receptor in breast cancer suggests novel therapeutic approaches. Cancer Res. 2008; 68: 5226-5235.
24. Callahan R, Egan SE. Notch signaling in mammary development and oncogenesis. J Mammary Gland Biol Neoplasia. 2004; 9: 145-163.
25. Dievart A, Beaulieu N, Jolicoeur P. Involvement of Notch1 in the development of mouse mammary tumors. Oncogene. 1999; 18: 5973-5981.
26. Miele L. Rational targeting of Notch signaling in breast cancer.

Expert Rev Anticancer Ther. 2008; 8: 1197-1202.
27. Sahlgren C, Gustafsson MV, Jin S, Poellinger L, Lendahl U. Notch signaling mediates hypoxia induced tumor cell migration and invasion. Proc Natl Acad Sci USA. 2008; 105: 6392-6397.
28. Soriano JV, Uyttendaele H, Kitajewski J, Montesano R. Expression of an activated Notch4(int-3) oncoprotein disrupts morphogenesis and induces an invasive phenotype in mammary epithelial cells in vitro. Int J Cancer. 2000; 86: 652-659.
29. Yun J, Pannuti A, Espinoza I, Zhu H, Hicks C, Zhu X et al. Crosstalk between PKCα and Notch4 in endocrine-resistant breast cancer cells. Oncogenesis. 2013; 2: e20
30. Lombardo Y, Faronato M, Filipovic A, Vircillo V, Magnani L, Coombes RC. Nicastrin and Notch4 drive endocrine therapy resistance and epithelial to mesenchymal transition in MCF7 breast cancer cells. Breast Cancer Res. 2014; 16: R62.
31. Kamakura S, Oishi K, Yoshimatsu T, Nakafuku M, Masuyama N, Gotoh Y. Hes binding to STAT3 mediates crosstalk between Notch and JAK-STAT signaling. Nat Cell Biol. 2004; 6: 547-554.
32. Clevenger CV. Roles and regulation of stat family transcription factors in human breast cancer. Am J Pathol 2004; 165: 1449-1460.
33. Lo HW, Cao X, Zhu H, Ali-Osman F. Constitutively activated Stat3 frequently coexpresses with epidermal growth factor receptor in high-grade gliomas and targeting STAT3 sensitizes them to iressa and alkylators. Clin Cancer Res. 2008; 14: 6042-6054.
34. Lo HW, Hsu SC, Xia W, Cao X, Shih JY, Wei Y et al. Epidermal growth factor receptor cooperates with signal transducer and activator of transcription 3 to induce epithelial-mesenchymal transition in cancer cells via up-regulation of twist gene expression. Cancer Res.

2007; 67: 9066-9076.
35. Knowlden JM, Hutcheson IR, Jones HE, Madden T, Gee JM, Harper ME et al. Elevated levels of epidermal growth factor receptor/c-erbB2 heterodimers mediate an autocrine growth regulatory pathway in tamoxifen-resistant MCF-7 cells. Endocrinology. 2003; 144: 1032-1044.
36. Gyorffy B, Lánczky A, Szállási Z (2012) Implementing an online tool for genome-wide validation of survival-associated biomarkers in ovarian-cancer using microarray data from 1287 patients. Endocr Relat Cancer 19(2):197-208.
37. Phuong NT, Kim SK, Im JH, Yang JW, Choi MC, Lim SC et al. Induction of methionine adenosyltransferase 2A in tamoxifen-resistant breast cancer cells. Oncotarget. 2016; 7: 13902-13916.
38. Rajendran S., Salwa S., Gao X., Tabirca S., O'Hanlon D., O'Sullivan GC et al. Murine bioluminescent hepatic tumour model. J Vis Exp. 2010; 41: e1977.
39. Soares KC, Foley K, Olino K, Leubner A, Skye C. Mayo SC et al. A preclinical murine model of hepatic metastases. J Vis Exp. 2014; 91: 51677.
40. Melchor JC, Rodriquez-Escudero FJ, Lujan S, Corcostegui B. Variation of estrogen and progesterone receptor status in breast cancer after tamoxifen therapy. Oncology. 1990; 47: 467-470.
41. Zhang X, Wang ZY. Estrogen receptor-α variant, ER-α36, is involved in tamoxifen resistance and estrogen hypersensitivity. Endocrinology. 2013; 154: 1990-1998.
42. Zhao Y, Deng C, Lu W, et al. Let-7 microRNAs induce tamoxifen sensitivity by downregulation of estrogen receptor α signaling in breast cancer. Mol Med. 2011; 17: 1233-1241.

43. Mangelsdorf DJ, Thummel C, Beato M, et al. The nuclear receptor superfamily: the second decade. Cell. 1995; 83: 835-839.
44. Wehling M. Specific, nongenomic actions of steroid hormones. Annu Rev Physiol. 1997; 59: 365-393.
45. Revankar CM, Cimino DF, Sklar LA, Arterburn JB, Prossnitz ER. A transmembrane intracellular estrogen receptor mediates rapid cell signaling. Science. 2005; 307: 1625-1630.
46. Kelly MJ, Levin ER. Rapid actions of plasma membrane estrogen receptors. Trends Endocrinol Metab. 2001; 12: 152-156.
47. Driggers PH, Segars JH. Estrogen action and cytoplasmic signaling pathways. Part II: the role of growth factors and phosphorylation in estrogen signaling. Trends Endocrinol Metab. 2002; 13: 422-427.
48. Zhang J, Li G, Li Z, et al. Estrogen-independent effects of ERα36 in ER-negative breast cancer. Steroids. 2012; 77: 666-673.
49. Bouris P, Skandalis SS, Piperigkou Z, Afratis N, Karamanou K, Aletras AJ et al. Estrogen receptor alpha mediates epithelial to mesenchymal transition, expression of specific matrix effectors and functional properties of breast cancer cells. Matrix Biol. 2015; 43: 42-60.
50. Lin SL, Yan LY, Liang XW, et al. A novel variant of ER-alpha, ER-alpha36 mediates testosterone-stimulated ERK and Akt activation in endometrial cancer Hec1A cells. Reprod Biol Endocrinol. 2009; 7: 102.
51. Al Saleh S, Al Mulla F, Luqmani YA. Estrogen receptor silencing induces epithelial to mesenchymal transition in human breast cancer cells. PLoS One. 2011; 6: e20610.
52. Yao K, Rizzo P, Rajan P, Albain K, Rychlik K, Shah S et al.

Notch1 and Notch4 receptors as prognostic markers in breast cancer. Int J Surg Pathol. 2011; 19: 607-613.
53. Harrison H, Farnie G, Howell SJ, Rock RE, Stylianou S, Brennan KR et al. Regulation of breast cancer stem cell activity by signaling through the Notch4 receptor. Cancer Res. 2010; 70: 709-718.
54. Marotta LL, Almendro V, Marusyk A, Shipitsin M, Schemme J, Walker SR et al. The JAK2/STAT3 signaling pathway is required for growth of CD44/CD24 stem cell-like breast cancer cells in human tumors. J Clin Invest. 2011; 121: 2723-2735.
55. Azare J, Leslie K, Al-Ahmadie H, Gerald W, Weinreb PH, Violette SM et al. Constitutively activated STAT3 Induces tumorigenesis and enhances cell motility of prostate epithelial cells through Integrin β6. Mol Cell Biol. 2007; 27: 4444-4453.
56. Snyder M, Huang XY, Zhang JJ. Identification of novel direct STAT3 target genes for control of growth and differentiation. J Biol Chem. 2008; 283: 3791-3798.
57. Darnell JE Jr. STATs and gene regulation. Science. 1997; 277: 1630-1635.
58. Kamran MZ, Patil P. Role of STAT3 in cancer metastasis and translational advances. Biomed Res Int. 2013; 2013: 421821.
59. Xie TX, Wei D, Liu M, Gao AC, Ali-Osman F, Sawaya R et al. STAT3 activation regulates the expression of matrix metalloproteinase-2 and tumor invasion and metastasis. Oncogene. 2004; 23: 3550-3560.
60. Saad S, Stanners SR, Yong R, Tang O, Pollock CA. Notch mediated epithelial to mesenchymal transformation is associated with increased expression of the Snail transcription factor. Int J Biochem Cell Biol. 2010; 42: 1115-1122.

61. Bergman MR, Cheng S, Honbo N, Piacentini L, Karliner JS, Lovett DH. A functional activating protein 1 (AP-1) site regulates matrix metalloproteinase 2 (MMP-2) transcription by cardiac cells through interactions with JunB-Fra1 and JunB-FosB heterodimers. Biochem J. 2003; 369: 485-496.
62. Philip S, Kundu GC. Osteopontin induces nuclear factor kappa B-mediated promatrix metalloproteinase-2 activation through I kappa B alpha/IKK signaling pathways, and curcumin (diferulolylmethane) down-regulates these pathways. J Biol Chem. 2003; 278: 14487-14497.
63. Clarke R, Dickson RB, Brfinner N: The process of malignant progression in human breast cancer. Ann Oncol. 1990; 1: 401-407.
64. Kalluri R, Weinberg RA. The basics of epithelial-mesenchymal transition. J Clin Invest. 2009; 119: 1420-1428.
65. Thiery JP, Acloque H, Huang RY, Nieto MA. Epithelial-mesenchymal transitions in development and disease. Cell. 2009; 139: 871-890.
66. Fearon ER. Connecting estrogen receptor function, transcriptional repression, and E-cadherin expression in breast cancer. Cancer cell. 2003; 3: 307-310.
67. Zheng X, Carstens JL, Kim J, Scheible M, Kaye J, Sugimoto H, Wu CC, LeBleu VS, Kalluri R. Epithelial-to-mesenchymal transition is dispensable for metastasis but induces chemoresistance in pancreatic cancer. Nature. 2015; 527: 525-530.
68. Fischer KR, Durrans A, Lee S, Sheng J, Li F, Wong ST et al. Epithelial-to-mesenchymal transition is not required for lung metastasis but contributes to chemoresistance. Nature. 2015; 527: 472-476.
69. Simoes B, O'Brien C, Eyre R, Silva A, Yu L, Sarmiento-Castro A

et al. Anti-estrogen resistance in human breast tumors is driven by Jag1-Notch4-dependent cancer stem cell activity. Cell Rep. 2015; 12: 1968-1977.
70. Noseda M, McLean G, Niessen K, Chang L, Pollet I, Montpetit R et al. Notch activation results in phenotypic and functional changes consistent with endothelial-to-mesenchymal transformation. Circ Res. 2004; 94: 910-917.
71. Chan KS, Sano S, Kiguchi K, Anders J, Komazawa N, Takeda J et al. Disruption of STAT3 reveals a critical role in both the initiation and the promotion stages of epithelial carcinogenesis. J Clin Invest. 2004; 114: 720-728.
72. De la Iglesia N, Konopka G, Puram SV, Chan JA, Bachoo RM, You MJ et al. Identification of a PTEN-regulated STAT3 brain tumor suppressor pathway. Genes Dev. 2008; 22: 449-462.
73. Aggarwal BB, Kunnumakkara AB, Harikumar KB, Gupta SR, Tharakan ST, Koca C et al. Signal transducer and activator of transcription-3, inflammation, and cancer: how intimate is the relationship? Ann N Y Acad Sci. 2009; 1171: 59-76.
74. Wen Z, Zhong Z, Darnell JE Jr. Maximal activation of transcription by STAT1 and STAT3 requires both tyrosine and serine phosphorylation. Cell. 1995; 82: 241-250.
75. Wen Z, Darnell JE Jr. Mapping of STAT3 serine phosphorylation to a single residue (727) and evidence that serine phosphorylation has no influence on DNA binding of STAT1 and STAT3. Nucleic Acids Res. 1997; 25: 2062-2067.
76. Hazan-Halevy I, Harris D, Liu Z, Liu J, Li P, Chen X et al. STAT3 is constitutively phosphorylated on serine 727 residues, binds DNA, and activates transcription in CLL cells. Blood. 2010; 115:

2852-2863.
77. Chung J, Uchida E, Grammer TC, Blenis J. STAT3 serine phosphorylation by ERK-dependent and -independent pathways negatively modulates its tyrosine phosphorylation. Mol. Cell Biol. 1997; 17: 6508-6516.
78. Turkson J. STAT proteins as novel targets for cancer drug discovery. Exp Opin Therap Targets. 2004; 8: 409-422.
79. Colomiere M, Ward AC, Riley C, Trenerry MK, Cameron-Smith D, Findlay J, Ackland L, Ahmed M. Cross talk of signals between EGFR and IL-6R through JAK2/STAT3 mediate epithelial-mesenchymal transition in ovarian carcinomas. Br J Cancer. 2009; 100: 134-144.
80. Wu J, Iwata F, Grass JA, Osborne CS, Elnitski L, Fraser P, Ohneda O, Yamamoto M, Bresnick EH. Molecular determinants of Notch4 transcription in vascular endothelium. Mol Cell Biol. 2005; 25: 1458-1474.
81. Li J, Tang Y, Cai D. IKKβ/NF-κB disrupts adult hypothalamic neural stem cells to mediate a neurodegenerative mechanism of dietary obesity and pre-diabetes. Nat Cell Biol. 2012; 14: 999-1012.
82. Kabos P, Haughian JM, Wang X, Dye WW, Finlayson C, Elias A, Horwitz KB, Sartorius CA. Cytokeratin 5 positive cells represent a steroid receptor negative and therapy resistant subpopulation in luminal breast cancers. Breast Cancer Res Treat. 2011; 128:45-55.
83. Haughiana JM, Pintoa MP, Harrell JC, Bliesner BS, Joensuu KM, Dye WW et al. Maintenance of hormone responsiveness in luminal breast cancers by suppression of Notch. PNAS. 2012; 109: 2742-2747.
84. Wang Z, Li Y, Ahmad A, et al. Targeting Notch signaling pathway to overcome drug resistance for cancer therapy. Biochim

Biophys Acta 1806: 258-267, 2010.
85. Purow B. Notch inhibition as a promising new approach to cancer therapy. Adv Exp Med Biol. 2012; 727: 305 - 319
86. Nicolas M, Wolfer A, Raj K, et al. Notch1 functions as a tumor suppressor in mouse skin. Nat Genet. 2003; 33:416 - 421.
87. Sriuranpong V, Borges MW, Ravi RK, et al. Notch signaling induces cell cycle arrest in small cell lung cancer cells. Cancer Res. 2001; 61: 3200 - 3205.
88. Zweidler-McKay PA, He Y, Xu L, et al. Notch signaling is a potent inducer of growth arrest and apoptosis in a wide range of B-cell malignancies. Blood. 2005; 106: 3898 - 3906.

국문초록

타목시펜 저항성 인간 유방암세포에서 ERα66/ERα36 및 Notch4/STAT3 경로를 통한 상피간엽이행 조절

부이 뚜 귀엔
지도교수: 강 건 욱

유방암은 가장 흔한 악성 종양 중 하나로 여성의 암으로 인한 사망률에 상당 부분을 차지한다. 유방암 종류 중 70%가 에스트로겐 수용체 알파(ERα) 양성이다. ERα 양성 유방암은 ERα 경로를 막아 호르몬 작용을 조절하는 치료 방법이 매우 효과적이며 그 중 타목시펜(TAM)이 가장 효과적인 약으로 주목 받아 왔다. 하지만 TAM에 오랜 시간 노출되면 초기 반응과 달리 유방암이 타목시펜 저항성을 갖게 된다. 이는 세포의 비정상적인 증식, 이동, 침윤, 전이를 촉진한다고 알려져 있다. 이전 보고에서 TAM 저항성 인간유래 유방암 세포(TAMR-MCF-7)가 parental 세포인 MCF-7 세포에 비해 mesenchymal marker 단백질의 발현이 증가 되어 있음을 밝혔다.

ERα은 66 kDa의 리간드 매개성 핵 수용체 전사인자이고, 인간 유방암에서 다양한 반응을 매개하는데 중요한 역할을 한다. 타목시펜 저항성 유방암(TAMR)의 형성 과정에서 ERα66의 하향 조절이 관여한다는

사실이 이미 보고된 바 있다. 최근 규명된 ERα36은 ERα66의 36 kDa의 새로운 이형으로 전사 활성 부분(AF-1과 AF-2)이 없지만 길이가 줄은 리간드 결합 부분과 ERα66과 동일한 DNA 결합 부분을 유지하고 있다. ERα66가 세포핵에 주로 분포하고 있는 반면, ERα36은 주로 세포질과 원형질막에 존재한다. MCF-7 세포와 다르게 TAMR-MCF-7 세포에서 ERα66의 발현은 감소하고 ERα36의 발현은 증가하였다. 본 연구에서 ERα66과 ERα36이 유방암에서 타목시펜 저항성 획득과 EMT 진행에서 갖는 역할을 평가하였다. ERα36의 과발현은 ERα66의 손실과 EMT를 진행시킨다. ERα36은 ERα66 발현을 억제하여 TAMR-MCF-7 세포에서 EMT 진행에 관여하는 것으로 추정된다. 하지만 쥐의 비장에 암을 주입하여 수행한 간 전이 평가 모델에서 ERα36이 과발현된 MCF-7은 세포의 외관 형질이 TAMR-MCF-7과 유사함을 보였지만 암의 전이를 일으키지 않았다. 또한, ERα66이 과발현된 TAMR-MCF-7은 상피세포 특이 인자인 E-cadherin의 복구를 통하여 간엽상피이행(mesenchymal epithelial transition, MET)을 일으킴을 확인하였다. 유사하게 ERα 음성 유방암세포인 MDA-MB-231과 SKBR3에서 ERα66의 과발현은 EMT와 세포 이동을 억제하였다. 하지만 비장 주입 간 전이 실험에서 대조군인 TAMR-MCF-7(TAMR-GFP) 세포 이식군과 ERα66 과발현 TAMR-MCF-7(TAMR-ER66)세포 이식군에서 동일한 간 전이 정도를 관찰할 수 있었다. 따라서 ERα36의 발현에 의하여 조절되는 ERα66은 분화와 정상 상피 구조를 유지하는데 중요한 역할을 한다. 더하여 ERα36은 에스트로겐 비의존성 세포 증식과 타목시펜 저항성 유방암 발생에 중요한 신호인자임을 본 연구에서 밝혔다.

Notch는 상피간엽이행(epithelial mesenchymal transition, EMT) 진행에 있어 암의 발달과 생장에 중요한 기능을 한다. Notch1과 Notch4

는 인간 유방암세포의 예후 인자로 보고되어 왔다. 본 논문에서 Notch1이 아닌 Notch4가 TAMR-MCF-7 세포에서 EMT 신호인자를 조절하는데 중요한 인자임을 밝혔다. Notch 저해제와 Notch4 siRNA로 Notch4를 억제시 EMT 마커 단백질의 발현이 감소하였다. STAT3 단백질은 암발생과 전이에 있어 중요한 신호 인자로 알려져 있다. TAMR-MCF-7 세포에서 STAT3 tyrosine 인산화가 지속적으로 증가하였으며, Notch 억제시 STAT3의 인산화가 억제됨을 발견하였다. 또한 immunoprecipitation-immunoblot 분석으로 STAT3가 Notch4 단백질 자체가 아닌 Notch4-세포내 부분(Notch4-ICD)과 물리적으로 결합되어 있음을 밝혔다. TAMR-MCF-7세포를 비장에 주입한 마우스 비장-간 전이 모델에서 N-[N-(3,5-Difluorophenacetyl)-L-alanyl]-S-phenylglycine t-butyl ester (DAPT, 10 mg/kg)를 복강내 투여한 마우스들은 비장에 암이 생성 되었으나 대조군에 비하여 간으로의 전이가 감소되었다. 본 연구는 STAT3와 Notch4-ICD가 물리적으로 결합되어 있고 이런 작용이 타목시펜 저항성 유방암에서 EMT 진행에 중요한 역할을 한다는 사실을 처음으로 규명하였다는 점에서 그 의미가 크다.

상기 결과들을 종합하여 본 연구에서는 타목시펜 저항성 유방암세포에서 상피간엽이행(EMT) 형질을 조절하는 핵심인자들로 Notch4/STAT3 신호와 ERα66/ERα36의 상대적 발현변화를 제시한다.

주요어: 상피간엽이행, ERα66, ERα36, Notch4, 타목시펜 저항성

학 번 : 2012-30773